

Electrical Resistivity of Silicate Glass Melts Calculation Based on the SciGlass Database

Alexander Fluegel*, David A. Earl, Arun K. Varshneya
New York State College of Ceramics; Alfred University; Alfred NY 14802; USA
**now with: Glassproperties.com; 07743 Jena; Germany*

Abstract

The relation between the chemical composition and the electrical resistivity (= 1/conductivity) of silicate glass melts at temperatures of 1000°C to 1400°C from the SciGlass Database was analyzed statistically. A model including ionic interactions was developed that permits calculating the glass melt electrical resistivity with a standard error of about 0.06 on the logarithmic resistivity scale in $\Omega \cdot \text{cm}$. The 95% confidence interval of the model prediction for industrial glasses in mass production largely depends on the composition of interest and the composition uncertainty, which can be quantified through software derived from this work.

Introduction

The electrical resistivity of glass melts is important for designing and operating electrical glass melting furnaces [1, 2]. It is the intention of this work to develop highly accurate predictions of electrical resistivity based on all available composition-resistivity data in the scientific literature.

Despite its high importance, few attempts have been made to calculate the electrical resistivity of glass melts based on their chemical composition. Often scientists and engineers refer to similar (and sometimes contradicting) data in the published literature or rely on time consuming and expensive experimental investigations. Only three advanced resistivity calculation methods exist to the authors' knowledge: the models by Mazurin and Prokhorenko [2], applicable to soda-lime and sodium borosilicate glass melts; the models by Hrma et al. and Vienna et al. [3, 4], applicable to special borosilicate glass melts used for nuclear waste vitrification; and the models by Fluegel et al. [5], applicable to various commercial soda-lime, borosilicate, and TV panel glass melts. The drawback of all the mentioned models is that they are based on experimental data from only one laboratory, which makes systematic errors possible [5]. Systematic comparisons to findings from other laboratories were not performed.

The paper by Fluegel et al. [5] also contains simple models for the binary and ternary systems $\text{SiO}_2\text{-Na}_2\text{O}$, $\text{SiO}_2\text{-K}_2\text{O}$, and $\text{SiO}_2\text{-Na}_2\text{O-CaO}$. Those simple models have no direct industrial application, but they use a high number of experimental values obtained for the mentioned systems from the scientific literature. This makes them accurate and valuable for "model calibration." No standard reference material for the electrical resistivity of glass melts has been established that could be used for calibration otherwise. The simple models by Fluegel et al. [5] are summarized in the Tables I to III and in Appendix (B).

Various glass melt electrical resistivity measurement techniques are not always comparable. In the following paragraphs, measurement techniques are briefly reviewed. The electrical resistivity ρ is defined as

$$\rho = R \cdot A / L \quad \text{Eq. (1)}$$

where A is the surface area of flat parallel electrodes, L is the distance between the electrodes, and R is the resistance. The unit of the resistivity or specific resistance is $\Omega \cdot \text{m}$ (or $\Omega \cdot \text{cm}$ in this paper). The conductivity or specific conductance κ is the reciprocal of the resistivity, $\kappa = 1/\rho$, with the unit $(\Omega \cdot \text{m})^{-1}$ or S/m ($S = \text{Siemens}$).

In glass melts, the electric current is predominantly transported through mobile ions. Other conducting species are not considered in this work. All measurements discussed in this paper were performed using alternating current (AC).

For accurate measurements of the electrical resistivity of glass melts, several details have to be considered. At the beginning of measurements, relatively low potential barriers occur for some conducting ions because of a broad potential barrier distribution caused by polarization effects in the electric field (ionic polarization). The conducting ions are capable of surmounting the low barriers easily, and the measured resistivity is relatively low. Eventually, as higher potential barriers appear for *all* conducting ions, the resistivity increases, and the constant steady-state resistivity is reached [2].

The conducting ions in the glass melt are discharged at the electrode surfaces, and insulating layers are formed, causing electrode polarization. The electrode polarization increases with decreasing AC frequency, i.e., the melt resistivity appears to increase as well with decreasing AC frequency up to about 2 kHz.

For obtaining resistivity data with reduced or negligible influence of electrode polarization effects, it is beneficial to record the electrical resistivity over various frequencies and to extrapolate to a constant resistivity value in the frequency-independent region at high frequency. However, the electrode polarization can never be totally avoided at glass-melting temperatures because ions are the predominantly conducting species in the glass melt, and electrons are the conducting species in the electrodes, i.e., surface reactions must always take place. Therefore, the electrode material influences the electrode polarization [6]. For glass melts, platinum electrodes are used most frequently in research at various frequencies, while less expensive molybdenum or tin oxide electrodes are used for industrial applications, often at 50 to 60 Hz.

The polarization-free resistivity of glass can be derived from the impedance-frequency spectrum by assuming equivalent circuits as described, for example, by Ravagnani et al. [7], Keding et al. [8], and Schiefelbein et al. [9].

Because the shape of the electric field during electrical resistivity measurements influences the result [9], a well-defined cell construction [10] is superior in principle to platinum-wire electrode techniques [2, 11-17].

The applied potential gradient during resistivity measurements of glass melts is not reported in several papers, unfortunately, despite its influence on the resistivity at high voltages because of various ionization potentials of the conducting ions [18-20]. Schiefelbein et al. [9] was using 30 to 60 mV.

Statistical data analysis

1) Source data handling

All experimental values in this work were obtained from original publications [2, 3, 11, 14-17, 21-24] and the SciGlass Database [25]. Data from several references are listed in Appendix (A) for convenience. The chemical glass compositions were converted to mol%. Among the equations used for describing the temperature dependence of the electrical resistivity of glass

melts [1, p 31], the Vogel-Fulcher-Tammann equation (VFT) was found to be accurate over the temperature range studied:

$$\log_{10}(\rho / \Omega \cdot \text{cm}) = A + B / (T - T_0) \quad \text{Eq. (2)}$$

where T is the temperature and A , B , and T_0 are composition-dependent parameters. However, these parameters are sensitive; their values can significantly change in response to small modifications of the data fitted. The parameters of the VFT equation only become relatively stable if experimental data in a temperature interval of several hundred °C are available, which is seldom the case, and even then, the measurement requires various techniques associated with additional errors (see ref. [5] for a discussion regarding glass viscosity).

To obtain maximum model accuracy with the available data, predictive models for the electrical resistivity of silicate glass melts were developed for three reference temperatures: 1000°C, 1200°C, and 1400°C.

Experimental resistivity data were interpolated, using Equation (2), to obtain $\log_{10}(\rho / \Omega \cdot \text{cm})$ at the three reference temperatures. The logarithmic scale is necessary for obtaining a constant error variance [26], i.e., for converting the relative error of resistivity measurements to an absolute error.

Because of the lack of an electrical resistivity standard glass, mean orientation values were established based on previously developed models for the systems $\text{SiO}_2\text{-Na}_2\text{O}$, $\text{SiO}_2\text{-K}_2\text{O}$, and $\text{SiO}_2\text{-CaO-Na}_2\text{O}$ [5]. The model source data and procedures are summarized in Appendix (B), and the mean orientation values (resistivities at reference temperatures) are listed in Tables I to III. The mean orientation values are based on a total of 400 experimental data from 47 references.

The mean orientation values, available in the systems $\text{SiO}_2\text{-Na}_2\text{O}$ and $\text{SiO}_2\text{-CaO-Na}_2\text{O}$ for all reference temperatures, and in $\text{SiO}_2\text{-K}_2\text{O}$ for 1400°C [5] were incorporated into the models in the same way as data-series by specific investigators, i.e., they were treated as experimental data. Based on initial model development, the limited data for multi-component glasses containing appreciable amounts of K_2O appeared inconsistent with the mean orientation values in the system $\text{SiO}_2\text{-K}_2\text{O}$ at 1000°C and 1200°C that were previously established as reliable. Therefore, coefficients for K_2O were determined using only the mean orientation values in the binary system $\text{SiO}_2\text{-K}_2\text{O}$ as described below.

Table I: Mean orientation values for the high-temperature electrical resistivity in the system $\text{SiO}_2\text{-Na}_2\text{O}$ (references in Appendix (B)), error = 95% confidence interval of the mean

C(Na_2O)		$\log(\rho/\Omega\cdot\text{cm})$ at T in $^\circ\text{C}$					
mol%	wt%	1000 $^\circ\text{C}$		1200 $^\circ\text{C}$		1400 $^\circ\text{C}$	
		Value	Error	Value	Error	Value	Error
16	16.42	0.974	0.038	0.710	0.068	0.512	0.064
17	17.44	0.895	0.035	0.635	0.062	0.441	0.061
18	18.46	0.821	0.033	0.565	0.057	0.374	0.058
19	19.48	0.751	0.031	0.498	0.054	0.311	0.056
20	20.50	0.685	0.030	0.436	0.052	0.252	0.055
21	21.52	0.623	0.029	0.377	0.051	0.197	0.054
22	22.54	0.565	0.028	0.323	0.051	0.145	0.054
23	23.55	0.510	0.028	0.271	0.051	0.097	0.053
24	24.57	0.459	0.028	0.223	0.051	0.052	0.053
25	25.59	0.412	0.028	0.178	0.051	0.010	0.053
26	26.60	0.367	0.028	0.136	0.052	-0.029	0.053
27	27.62	0.326	0.028	0.097	0.052	-0.066	0.053
28	28.63	0.287	0.029	0.061	0.053	-0.100	0.054
29	29.64	0.250	0.030	0.027	0.054	-0.131	0.054
30	30.66	0.217	0.031	-0.004	0.055	-0.161	0.055
31	31.67	0.185	0.032	-0.034	0.056	-0.188	0.056
32	32.68	0.156	0.034	-0.061	0.058	-0.213	0.058
33	33.69	0.128	0.035	-0.087	0.060	-0.237	0.059
34	34.70	0.102	0.036	-0.111	0.061	-0.258	0.061
35	35.71	0.078	0.038	-0.133	0.063	-0.279	0.063
36	36.72	0.055	0.039	-0.154	0.065	-0.298	0.064
37	37.73	0.033	0.040	-0.174	0.066	-0.316	0.066
38	38.73	0.012	0.041	-0.193	0.068	-0.333	0.068
39	39.74	-0.007	0.041	-0.211	0.069	-0.349	0.070
40	40.75	-0.027	0.041	-0.228	0.069	-0.365	0.071

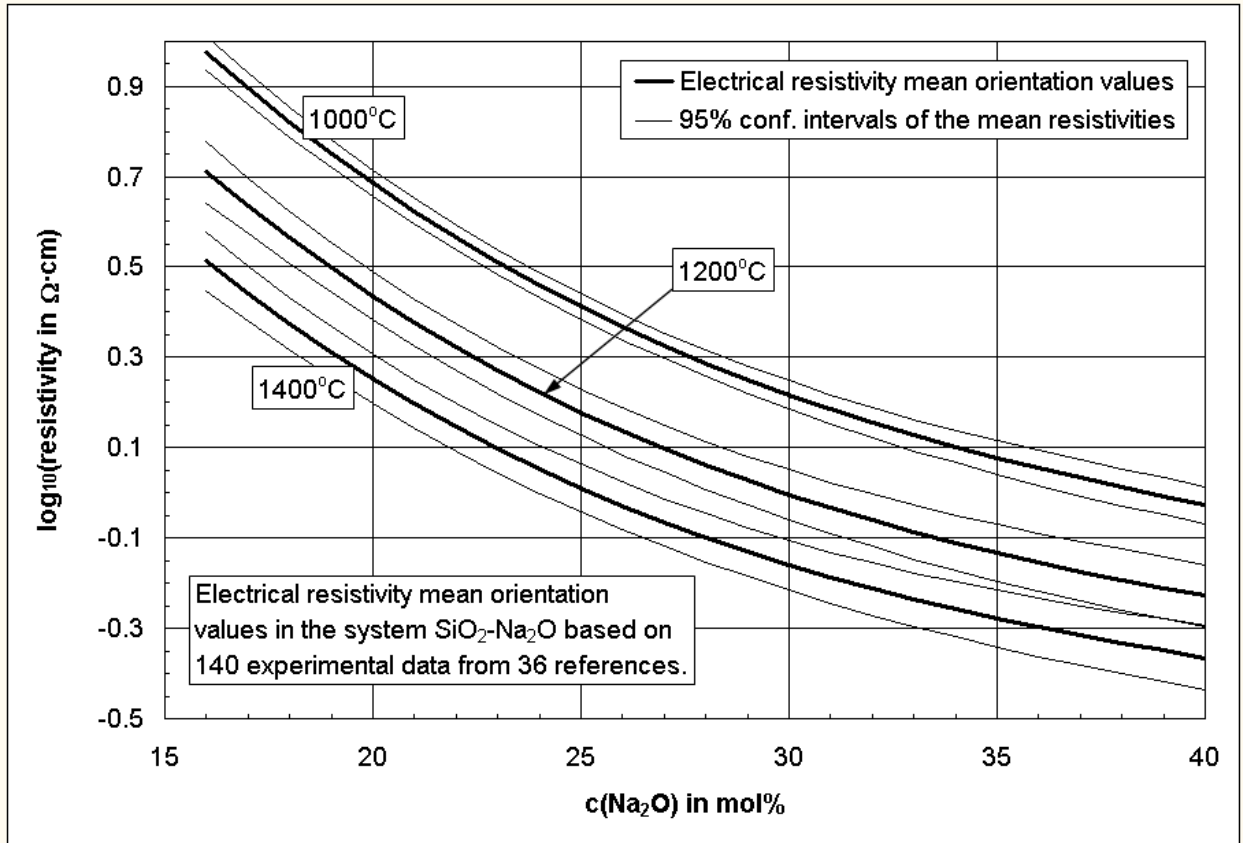


Figure 1: High-temperature electrical resistivity mean orientation values from Table I

Table II: Mean orientation values for the high-temperature electrical resistivity in the system $\text{SiO}_2\text{-K}_2\text{O}$ (references in Appendix (B)), error = 95% confidence interval of the mean

C(K_2O)		$\log(\rho/\Omega\cdot\text{cm})$ at T in $^\circ\text{C}$					
mol%	wt%	1000 $^\circ\text{C}$		1200 $^\circ\text{C}$		1400 $^\circ\text{C}$	
		Value	Error	Value	Error	Value	Error
16	16.42	1.139	0.035	0.883	0.061	0.692	0.060
17	17.44	1.066	0.033	0.811	0.059	0.621	0.058
18	18.46	0.997	0.032	0.742	0.057	0.552	0.056
19	19.48	0.931	0.031	0.677	0.056	0.488	0.055
20	20.50	0.869	0.030	0.615	0.054	0.426	0.056
21	21.52	0.810	0.029	0.557	0.053	0.368	0.056
22	22.54	0.754	0.029	0.502	0.053	0.314	0.056
23	23.55	0.702	0.029	0.450	0.053	0.263	0.057
24	24.57	0.651	0.029	0.401	0.053	0.215	0.057
25	25.59	0.604	0.030	0.355	0.055	0.171	0.058
26	26.60	0.558	0.031	0.311	0.056	0.129	0.058
27	27.62	0.515	0.032	0.271	0.059	0.091	0.059
28	28.63	0.473	0.034	0.232	0.062	0.056	0.061
29	29.64	0.433	0.036	0.197	0.064	0.025	0.063
30	30.66	0.395	0.039	0.163	0.068	-0.004	0.066
30	31.67	0.358	0.041	0.132	0.071	-0.029	0.070
32	32.68	0.322	0.043	0.103	0.075	-0.051	0.076

Table III: Mean orientation values for the high-temperature electrical resistivity in the system $\text{SiO}_2\text{-CaO-Na}_2\text{O}$ (references in Appendix (B)), error = 95% confidence interval of the mean

C(CaO)		C(Na ₂ O)		log($\rho/\Omega\cdot\text{cm}$) at T in °C					
mol%	wt%	mol%	wt%	1000°C		1200°C		1400°C	
				Value	Error	Value	Error	Value	Error
5	4.65	21	21.59	0.682	0.017	0.409	0.029	0.200	0.035
5	4.65	23	23.63	0.580	0.018	0.317	0.030	0.118	0.037
5	4.65	25	25.67	0.493	0.021	0.238	0.034	0.048	0.039
7	6.53	15	15.47	1.093	0.018	0.773	0.031	0.518	0.036
7	6.53	17	17.52	0.946	0.014	0.639	0.023	0.396	0.031
7	6.52	19	19.57	0.817	0.016	0.522	0.025	0.291	0.032
7	6.52	21	21.62	0.705	0.018	0.421	0.029	0.202	0.035
7	6.52	23	23.66	0.608	0.021	0.335	0.033	0.126	0.039
7	6.51	25	25.71	0.525	0.024	0.262	0.038	0.064	0.045
9	8.41	15	15.49	1.104	0.016	0.768	0.026	0.498	0.032
9	8.41	17	17.55	0.961	0.017	0.640	0.028	0.384	0.032
9	8.40	19	19.60	0.836	0.020	0.529	0.033	0.286	0.036
9	8.39	21	21.65	0.729	0.024	0.433	0.039	0.203	0.042
9	8.39	23	23.70	0.636	0.028	0.353	0.046	0.135	0.050
9	8.38	25	25.74	0.558	0.034	0.286	0.053	0.079	0.058
11	10.29	15	15.51	1.114	0.020	0.764	0.034	0.478	0.036
11	10.29	17	17.57	0.976	0.022	0.641	0.037	0.371	0.037
11	10.28	19	19.63	0.856	0.026	0.535	0.044	0.280	0.043
11	10.27	21	21.68	0.752	0.031	0.446	0.051	0.205	0.051
11	10.27	23	23.73	0.664	0.037	0.371	0.060	0.143	0.062
13	12.18	15	15.53	1.124	0.026	0.759	0.045	0.459	0.042
13	12.17	17	17.59	0.990	0.028	0.642	0.048	0.358	0.044
13	12.17	19	19.65	0.875	0.032	0.542	0.055	0.274	0.051
13	12.16	21	21.71	0.776	0.038	0.458	0.064	0.206	0.062
13	12.15	23	23.76	0.692	0.046	0.389	0.075	0.152	0.075
15	14.07	15	15.55	1.134	0.033	0.754	0.058	0.439	0.050
15	14.07	17	17.62	1.005	0.034	0.643	0.061	0.345	0.053
15	14.06	19	19.68	0.894	0.039	0.549	0.068	0.269	0.061
15	14.05	21	21.74	0.799	0.046	0.471	0.077	0.207	0.074

For all remaining multi-component glasses summarized in the SciGlass database [25], datasets were excluded from further calculations if it was not possible to obtain resistivity values at 1000, 1200, and 1400°C by interpolation from data. Also, some publications were not considered if they contained only too few measurements (one to five). All references and part of the source data are given in Appendices (A) and (B).

Next, initial modeling tests were performed to evaluate the consistency of all available experimental values. The data-series by Loryan et al. [27] in the ternary system $\text{SiO}_2\text{-B}_2\text{O}_3\text{-Al}_2\text{O}_3$ was excluded because electrical resistivities were not studied by any other investigator for those special compositions and fitting the data appeared difficult. The initial modeling studies showed that resistivities of those glasses that do not contain modifying oxides (e.g., Na_2O , CaO , K_2O ,

MgO, BaO, SrO, H₂O, PbO) may require a complete change of the modeling technique, which did not appear reliable based on results of only one investigator. The data-series by Saringyulyan et al. [28] of lead-silicate glasses with up to 50 mol% PbO (Table XVI in Appendix (A)) were excluded because of their special compositions, while values by Saringyulyan et al. in the binary system SiO₂-K₂O were still considered [5]. The data-series by Verzhkhovskaya [29] were excluded because several outliers occurred that could not be related to unique compositions investigated. Inconsistent data prevented the use of experimental values in the publication by Startsev [13], e.g., a "Float" and "Fourcault" glass had significantly different properties despite very similar compositions. The same applies to a borosilicate glass "8486" in ref. [22], which allegedly shows unusually different behavior to similar compositions in the same paper. The early publication by Endell et al. [30] was excluded because the reported resistivity values are up to ten thousand times higher than comparable data of other investigators.

In total, the models in this work consider more than 1100 experimental data from 53 references. Most electrical resistivity values used in this study are summarized by Mazurin et al. [2], Varshneya et al. [16] and Fluegel et al. [5].

2) Modeling procedure [31-37]

Details of the modeling technique are described in a separate paper [26]. The model is based on a third-order polynomial function:

$$\log(\rho) = \beta_0 + \sum_{i=1}^n \left(\beta_i C_i + \sum_{k=i}^n \left(\beta_{ik} C_i C_k + \sum_{m=k}^n \beta_{ikm} C_i C_k C_m \right) \right) \quad Eq. (3)$$

where β_0 is the *intercept*, β_i , β_{ik} , and β_{ikm} are the i^{th} component first-order coefficient, ik^{th} component second-order coefficient, and ikm^{th} component third-order coefficient, respectively, C_i is the i^{th} component concentration in mol%, and n is the number of significant components.

Equation (3) was fitted to $\log(\rho/(\Omega \cdot \text{cm}))$ at 1000°C, 1200°C, and 1400°C. Systematic trends and offsets (block-effects) in specific data-series were analyzed with "categorical" or "dummy" variables [26, 31, 32, 35]. Possible reasons for block-effects are differences in the experimental conditions (thermal glass history, measurement frequency, voltage, electrode material, different composition areas), or systematic errors of specific investigators. Most experimental conditions were not considered as model variables because of the lack of data. The uneven coverage of the investigated composition region was mitigated by applying leverage analysis [26] (e.g., values by Saringyulyan in Table XVI were not modeled).

Based on the linear correlations (Pearson's matrix) [26] between all variables (concentrations, concentration products, and dataset-specific dummy variables) were evaluated. Strongly correlated terms were excluded from further calculations. The correlation matrices are given in ref. [38].

The fitting method was ordinary least-squares and variable significance was determined through t-tests (Table V) via forward selection [26]. Outlying datapoints were detected through standardized and externally studentized residuals [26], and successively excluded from the calculations. Variance-covariance matrices [26] are summarized in ref. [38].

The coefficients for K₂O at 1000°C and 1200°C were forced to fit the mean orientation values in Table II because the few remaining experimental data of glasses containing high amounts of K₂O did not result in meaningful model predictions for the binary system SiO₂-K₂O.

Goodness of fit indicators R^2 , R^2 (adjusted), and R^2 (predicted) were used as well as the model standard error (Table VI) and a comparison of the model standard error with the experimental error. According to the high R^2 (predicted) values, it did not appear informative to perform a model validation procedure through data-splitting [26]; i.e., data-splitting must lead to very similar R^2 values as given in Table VI based on the lack of high-leverage datapoints [26]. The final validation of the model itself requires well-planned follow-up experiments in the future, and establishing a standard reference material for electrical resistivity in glass similar to viscosity standards.

Model application limits (concentration limits and component-combination limits) are calculated automatically from the source data and the composition of interest in ref. [38], following the procedure explained in ref. [26]. Predictions are possible through the coefficients in Table IV using Equation (3) and considering the concentration limits, or through ref. [38]. A property calculation example is shown below. The standard confidence intervals of the mean model prediction can be derived as described in a previous article [26], or through ref. [38]. The influence of the glass composition uncertainty on the prediction error may be quantified using ref. [38] according to equations in ref. [26].

Modeling results

Table IV displays the model coefficients, and further statistical indicators are seen in Tables V and VI. Excluded statistically insignificant variables that have no certain influence in the result are not shown in Tables IV and V. The standard errors of the coefficients in Table IV can be determined by dividing the coefficient by its corresponding t-value in Table V. The concentration limits and important component combination limits that must be taken into account during model application can be evaluated using the electrical resistivity calculator connected to this publication [38]. The calculator also estimates the confidence intervals of the model predictions, considering the model and glass composition uncertainties.

Table IV: Electrical resistivity model coefficients based on the glass composition in mol%, model result in $\log_{10}(\rho/\Omega\cdot\text{cm})$ at specified temperature, excluded insignificant variables not mentioned

Variables	Coefficients		
	1000°C	1200°C	1400°C
Intercept	2.84198	2.41516	1.79516
B₂O₃	0.00837	0	0
Al₂O₃	0.07117	0.04730	0.01838
Li₂O	-0.09614	-0.09017	-0.07401
Na₂O	-0.18391	-0.16245	-0.11008
(Na₂O)²	0.004844	0.003874	0.001807
(Na₂O)³	-0.0000524	-0.0000374	-0.0000104
K₂O	-0.14530	-0.12087	-0.05532
(K₂O)²	0.002760	0.001593	-0.001657
(K₂O)³	-0.0000212	-0.0000022	0.0000499
MgO	0.01529	0.00516	0
CaO	0.02759	0	-0.00614
(CaO)²	0	-0.000380	-0.000503
SrO	0.01648	0.00519	-0.00360
BaO	0.03265	0	-0.00854
ZrO₂	0.11009	0.03420	0
ZnO	-0.00974	-0.01436	-0.01499
PbO	0.01396	0	-0.00970
B₂O₃*Al₂O₃	-0.006400	-0.004637	-0.002288
B₂O₃*K₂O	0.009835	0.005114	0.001709
B₂O₃*MgO	0.001413	0.001891	0.001399
Al₂O₃*Li₂O	-0.006459	-0.002965	0
Al₂O₃*Na₂O	-0.003263	-0.001979	-0.000631
Al₂O₃*K₂O	-0.001344	-0.000627	0
Li₂O*Na₂O	0.003791	0.003385	0.002441
Li₂O*K₂O	0.006357	0.005200	0.003822
Li₂O*CaO	-0.004558	-0.003209	-0.002514
Na₂O*K₂O	0.007281	0.005861	0.002823
Na₂O*MgO	-0.001447	-0.000975	-0.000584
Na₂O*CaO	-0.000994	0.000510	0.000754
K₂O*CaO	0.000288	0.001641	0.001607
Na₂O*K₂O*CaO	0.000332	0.000161	0
Varshneya et al. [16], Trend	0	0.056	0.136
Kim et al. [14], Offset	0	0	0.130

Table V: *t*-values of the model coefficients in Table IV

Variables	t-values		
	1000°C	1200°C	1400°C
B_2O_3	7.31	/	/
Al_2O_3	10.31	8.77	5.77
Li_2O	-23.29	-25.47	-21.33
Na_2O	-56.80	-62.32	-20.79
$(Na_2O)^2$	20.24	19.52	6.93
$(Na_2O)^3$	-12.02	-10.19	-2.57
K_2O	Coefficients for K_2O were incorporated into the models as constants.		-9.01
$(K_2O)^2$			-3.71
$(K_2O)^3$			5.29
MgO	11.32	4.58	/
CaO	12.62	/	-2.51
$(CaO)^2$	/	-7.26	-6.27
SrO	7.50	2.99	-2.22
BaO	7.81	/	-2.91
ZrO_2	7.54	3.47	/
ZnO	-5.16	-9.01	-10.45
PbO	4.05	0.00	-3.52
$B_2O_3*Al_2O_3$	-13.87	-12.84	-7.16
$B_2O_3*K_2O$	9.60	5.81	2.06
B_2O_3*MgO	2.76	4.67	3.81
$Al_2O_3*Li_2O$	-3.04	-1.75	/
$Al_2O_3*Na_2O$	-9.27	-7.20	-3.68
$Al_2O_3*K_2O$	-4.07	-2.44	/
Li_2O*Na_2O	8.12	8.49	7.33
Li_2O*K_2O	13.66	13.03	10.39
Li_2O*CaO	-4.04	-3.30	-3.04
Na_2O*K_2O	34.44	38.07	9.17
Na_2O*MgO	-10.16	-8.29	-7.08
Na_2O*CaO	-6.97	6.73	6.74
K_2O*CaO	1.70	14.90	13.05
Na_2O*K_2O*CaO	7.82	4.42	/
Varshneya et al. [16], Trend	/	6.32	12.01
Kim et al. [14], Offset	/	/	6.21

Table VI: Further statistical indicators*

	Model at T in °C		
	1000°C	1200°C	1400°C
Model standard error	0.0649	0.0557	0.0497
R²	0.9957	0.9953	0.9878
R ² , adjusted	0.9953	0.9950	0.9866
R ² , predicted	0.9940	0.9944	0.9743
Standard deviation of residuals	0.0620	0.0535	0.0476
Number of data in model	301	314	312
Degree of freedom	274	289	284
Observation minimum	-0.1300	-0.3200	-0.4500
Observation average	1.2574	0.8793	0.6018
Observation maximum	4.3900	2.7030	1.7910
Observation std. deviation	0.7096	0.5520	0.4296

*Predictions and confidence intervals can be determined using an electrical resistivity calculator [38].

The electrical resistivity curve between 1000°C and 1400°C can be derived from the resistivity reference points modeled through Table IV, or ref. [38]. The resistivity values in $\log(\rho/\Omega\cdot\text{cm})$ at $T = 1000^\circ\text{C}$, 1200°C , and 1400°C ($\log(\rho_{1000})$, $\log(\rho_{1200})$, $\log(\rho_{1400})$) need to be inserted into the Equations (4) to (6) to calculate the Vogel-Fulcher-Tammann constants (A , B , T_0), which in turn give the resistivity-temperature curve through Equation (2):

$$T_0 = 200 \frac{7 \log(\rho_{1400}) + 5 \log(\rho_{1000}) - 12 \log(\rho_{1200})}{\log(\rho_{1400}) + \log(\rho_{1000}) - 2 \log(\rho_{1200})} \quad \text{Eq. (4)}$$

$$B = [\log(\rho_{1000}) - \log(\rho_{1200})](T_0 - 1000)(T_0 - 1200) / 200 \quad \text{Eq. (5)}$$

$$A = \frac{B + (T_0 - 1200) \log(\rho_{1200})}{T_0 - 1200} \quad \text{Eq. (6)}$$

Calculation example: The electrical resistivity of a glass melt needs to be determined with the following composition in mol%: 73.7 SiO₂, 5.81 Na₂O, 9.68 K₂O, 10.8 CaO. The coefficients in Table I, multiplied with the concentrations in mol%, result in the electrical resistivity values after adding the appropriate model intercepts:

$\log(\rho/\Omega\cdot\text{cm})$ at **1000°C**:

$$2.84198 - 5.81 \times 0.18391 + (5.81)^2 \times 0.004844 - (5.81)^3 \times 0.0000524 - 9.68 \times 0.1453 + (9.68)^2 \times 0.00276 - (9.68)^3 \times 0.0000212 + 10.8 \times 0.02759 + 5.81 \times 9.68 \times 0.007281 - 5.81 \times 10.8 \times 0.000994 + 9.68 \times 10.8 \times 0.000288 + 5.81 \times 9.68 \times 10.8 \times 0.000332 = \mathbf{1.64} = \log(\rho_{1000})$$

The values of $\log(\rho)$ at 1200°C and 1400°C are 1.16 and 0.82 respectively. The calculated decadic logarithms of the electrical resistivities in $\Omega\cdot\text{cm}$ at 1000°C, 1200°C, and 1400°C compare well with experimental data in Table VIII and Figure 2. With these values, Equations (4) to (6) yield $T_0 = 28.57^*$, $B = 2731.1$, and $A = -1.171$. Hence, the complete VFT equation is:

* This value of T_0 appears rather low for scientific interpretation. However, the VHT equation is only used in this work to describe electrical resistivity data within the examined temperature range of 1000 to 1400°C.

$\log_{10}(\rho/\Omega\cdot\text{cm}) = -1.171 + 2731.1 / (T \text{ in } ^\circ\text{C} - 28.57)$. The obtained resistivity curve, depicted in Figure 2, should not be extended beyond the 1000 to 1400°C temperature interval because it would exceed the model application limits in this work. Especially at low temperatures, crystallization and phase separation might occur that can change the electrical resistivity significantly.

Next, it is possible to fit the determined values to the Vogel-Fulcher-Tammann (VFT) equation (Equation (2)) with common mathematics programs, or reference [38]. In case such a program is not available, the Equations (4) to (6) can be used as an alternative.

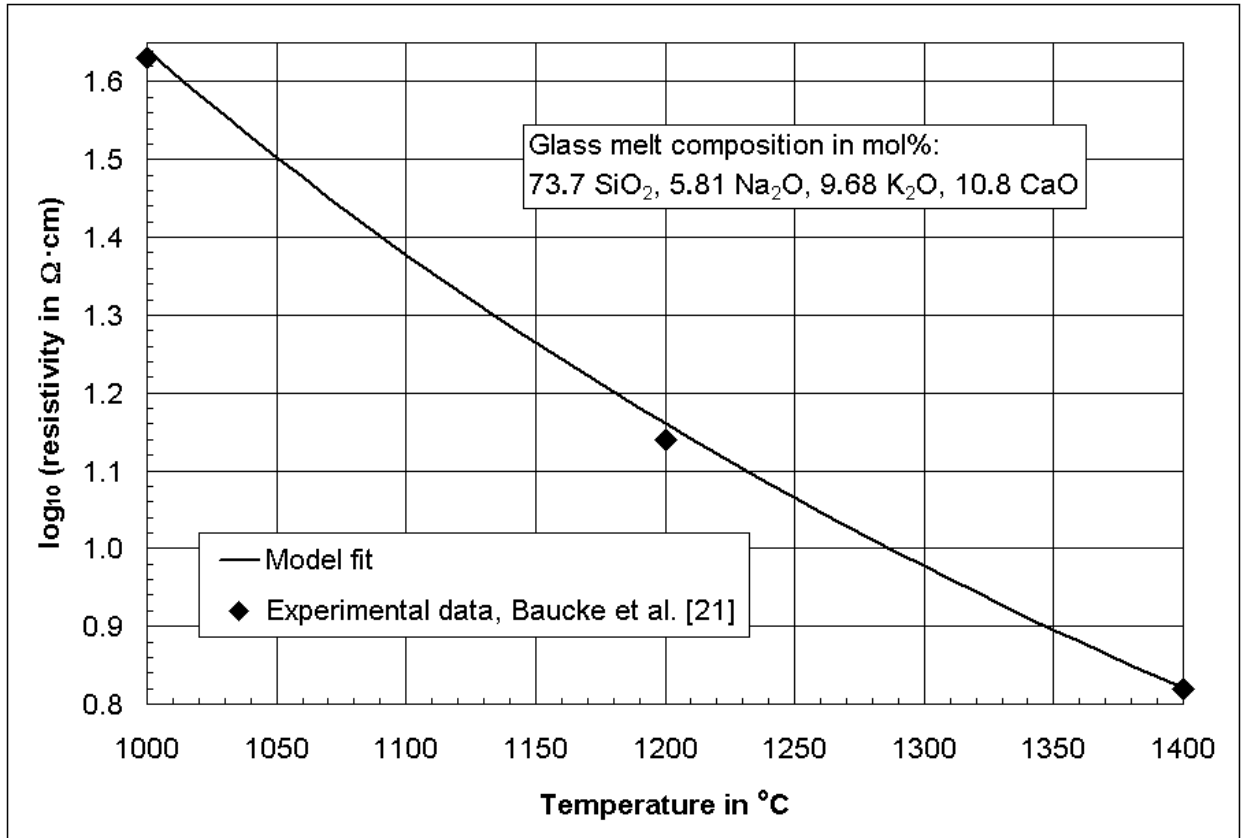


Figure 2: Example resistivity curve

The degree of model scatter (residual scattering) at 1000°C is depicted graphically in Figure 3. The model scatter at 1200°C and 1400°C is similar. Panel 11 in Figure 3 shows patterning because it represents the residuals of the regularly arranged orientation values in Table I to III. Table VII lists the standard deviations σ of part of the scatter data (residuals). Table VII also shows a comparison of the precision of previous models based on a single reference [5] with the accuracy of the models in this study using the standard deviation of the model residuals.

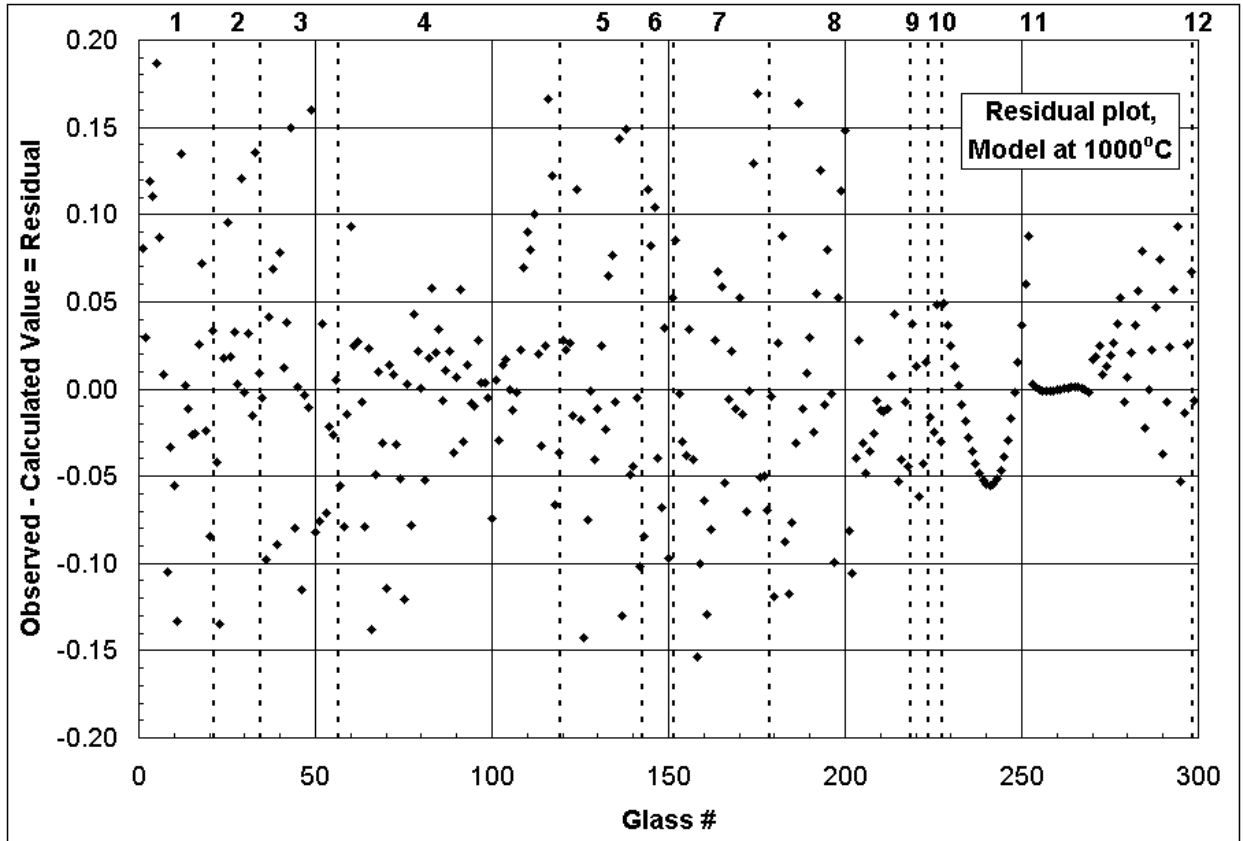


Figure 3: Residual plot of model at 1000°C: 1 – TV panel glasses [16], 2 – Textile fiber E glasses [16], 3 – Low-expansion borosilicate glasses [16], 4 – Soda-lime container and float glasses [2, 16], 5 – Wool fiber glasses [16], 6 – Ternary sodium borosilicates [2], 7 – Glasses with high levels of alkaline earth oxides and zinc oxide [17], 8 – Mixed alkali glasses [11, 14, 21, 24], 9 – High alumina glasses [23], 10 – Glasses for nuclear waste immobilization [3, 5], 11 – From left to right: mean orientation values in the systems $\text{SiO}_2\text{-Na}_2\text{O}$, $\text{SiO}_2\text{-K}_2\text{O}$, and $\text{SiO}_2\text{-CaO-Na}_2\text{O}$ given in Tables I to III [5], 12 – retracted standard NIST 1414 [15]; data in model by Pfeiffer [22] not shown in Figure 3 to maintain readability

Table VII: Precision and accuracy comparison (standard deviation σ of the model residuals in $\log_{10}(\rho/\Omega \cdot \text{cm})$), previous models based on a single reference and model in this study based on 53 references

Glass type, investigator	σ , model based on single reference at T in °C [5]			σ , model in this study based on 53 references at T in °C		
	1000°C	1200°C	1400°C	1000°C	1200°C	1400°C
TV panel glasses, Varshneya et al. [16]	0.0507	0.0394	0.0348	0.083	0.056	0.046
Textile fiber E glasses, Varshneya et al. [16]	0.2405	0.1374	0.0939	0.070	0.095	0.069
Low-expansion borosilicate glasses, Varshneya et al. [16]	0.0734	0.0651	0.0617	0.075	0.065	0.050
Soda-lime container and float glasses, Varshneya et al. [16]	0.0217	0.0248	0.0212	0.047	0.042	0.037
Wool fiber glasses, Varshneya et al. [16]	0.0546	0.0479	0.0490	0.077	0.059	0.053
Glasses for nuclear waste immobilization, Vienna et al [3], see also ref. [5]*	/	0.0342	/	0.036	0.047	0.015
High-alumina glasses, Kirakosyan et al. [23]	/	/	/	0.042	0.034	0.036
Mixed alkali glasses, Baucke et al. [21], Tickle [11], Kim et al. [14], Kostanyan et al. [24]	/	/	/	0.069	0.050	0.051
Glasses with high levels of alkaline earth oxides and zinc oxide, Mazurina et al. [17]	/	/	/	0.073	0.074	0.066
Systems SiO ₂ -Na ₂ O, SiO ₂ -K ₂ O, and SiO ₂ -CaO-Na ₂ O [5]	/	/	/	0.036	0.016	0.021

* In this study, only those five glasses for waste immobilization reported by Vienna et al. [3] were considered that could be extrapolated over the full temperature range of 1000 to 1400°C.

Discussion

Modeling approach

The multiple regression slack-variable modeling technique using polynomial functions appears to describe the electrical resistivity data well for most silicate glasses. The R^2 values and standard errors in table VI are reasonable, compared with previous studies [4, 5]. Some high-lead silicate glasses reported by Saringyulyan et al. (Table XVI [28]) did not fit well in this work either because of inaccurate measurements or because the composition area has not yet been investigated by several investigators. The resistivity values reported by Loryan et al. [27] in the ternary system SiO₂-B₂O₃-Al₂O₃ (no modifying oxides) are systematically higher than the model in this work suggests. It might be necessary in future to modify the modeling technique if the special compositions by Loryan et al. have to be considered. Again, it would be beneficial if several investigators contributed their data for establishing accuracy.

Over- and under-fitting of the models was prevented in this work by using the t-values as a measure of variable significance. The standard error of the models is higher than the measurement precision [5]; i.e., no over-fitting occurred. The similarity between the R^2 and the adjusted R^2 values in Table VI shows that the model did not include insignificant variables.

Phase separation and crystallization may lead to significant property changes even if the overall glass composition remains constant. Therefore, compositions that show phase separation and/or crystallization would appear as outliers based on the model in this paper.

Model accuracy

Among the 53 references considered, only 2 seemed to show systematic differences from others (Table IV). In addition, the data-series by Baucke et al. [21], which is based on a very reliable measurement technique, did not show any systematic differences within the error limits. The good agreement between the R^2 and predicted R^2 values in Table VI demonstrates that the model did not include high-leverage datapoints that could lead to inaccurate predictions.

It is important to be aware of the fact that one of the data-series that appears to be systematically different from others is very large (Varshneya et al. [16], 134 datasets outlier not considered) and therefore influential. It was already mentioned [5] that the electrical resistivity of the soda-lime container and float glasses by Varshneya et al. did compare well to a series by Mazurin et al. [2] and to mean orientation values in the systems $\text{SiO}_2\text{-Na}_2\text{O}$, $\text{SiO}_2\text{-K}_2\text{O}$, and $\text{SiO}_2\text{-CaO-Na}_2\text{O}$ [5] at 1000°C and at 1200°C ; however, disagreement occurred at 1400°C . In the present work, further studies were performed, e.g., the soda-lime container and float glasses by Varshneya et al. were compared to Baucke et al. [21], and the complete series by Varshneya et al. was compared to mean orientation values in the systems $\text{SiO}_2\text{-Na}_2\text{O}$, $\text{SiO}_2\text{-K}_2\text{O}$, and $\text{SiO}_2\text{-CaO-Na}_2\text{O}$. It always appeared that at 1400°C , the electrical resistivity data by Varshneya et al. are slightly too high, approximately 14% as seen in Table IV. Systematic errors within other data-series (Table IV) are by far less influential because of the smaller size of those series.

It is surprising that the series by Kostanyan et al. [24] seems to be in good agreement with other data, even though the low measurement frequency of 50 Hz (Table XV) must lead to electrode polarization effects.

It should be noted that systematic errors during electrical resistivity measurements of glass melts are not unusual because a reliable technique similar to Schiefelbein et al. [9] or Baucke et al. [10] is not yet well-established. It is even stated in the publication by Schiefelbein et al. [9] that most electrical resistivity measurements of liquids are, "by and large, inaccurate." The authors of the present paper would like to suggest, instead, that most previous electrical resistivity data of glass melts are only less accurate, i.e., a precision and accuracy can be evaluated that may be improved in the future. Previous electrical resistivity data can be a basis for model predictions.

The offset and trend variables in Table IV correct most systematic errors, i.e., the overall modeling result can be considered as accurate as the source data allow. More precisely, the model accuracy can be assumed to be close to the standard confidence intervals of the mean model prediction, which may be determined using the electrical resistivity calculator based on this work [38].

The model includes the majority of experimental data from scientific publications available at the time of the model creation in 2005. However, it can not be ruled out that future experimental findings could make significant modifications of this model necessary. The user should be

cautious, especially about predictions in glass composition areas where few experimental data exist in the literature.

Figure 3 shows that for the model at 1000°C, the residuals (difference of observed and calculated values) in the system SiO₂-K₂O are very close to zero because the models at 1000°C and at 1200°C were adjusted to those values, as described above. In the systems SiO₂-Na₂O and SiO₂-Na₂O-CaO, larger differences occur. It appears possible that in the systems SiO₂-Na₂O and SiO₂-Na₂O-CaO, the accuracy of the mean orientation values in Tables I to III might be slightly superior to this study. Further experimental data are required for a detailed evaluation.

In view of the fact that the mean orientation values in the systems SiO₂-Na₂O, SiO₂-K₂O, and SiO₂-CaO-Na₂O [5] were included into the models in this work as modeling results, i.e., the original literature data were modeled two times, they fit relatively well. The error propagation for the two-step modeling method for the mean orientation values was not considered for accuracy predictions in this work. In future, systematic measurement results in simple glass-forming systems based on reliable techniques should be modeled directly without applying a two-step modeling procedure.

Besides the present study and Fluegel et al. [5], the number of publications about the modeling of the electrical resistivity of glass melts is very limited. Models by Hrma et al. and Vienna et al. [3, 4] are valid specifically for glasses used for nuclear waste immobilization. Mazurin and Prokhorenko published a model for soda-lime glass melts [2]; however, it is based on significantly less data than used in the present study. It becomes obvious that future electrical resistivity measurements would be very beneficial for improving the model accuracy.

Model precision

It can be concluded from the data in Table VII that the precision of models that are based on just one reference is often comparable with the accuracy of models based on several references. The only exception might be soda-lime glasses where the precision is clearly higher following ref. [5] than in this study. However, it should be noted that a high precision does not guarantee the absence of systematic errors, i.e., in many cases, the accuracy is more important than the precision because systematic errors are considered. In other words, highly repeatable findings of one investigator might be sometimes inaccurate systematically, but the overall systematic error of several investigators can be assumed to be close to zero on average.

Sometimes inaccurate measurements can be valuable if the precision is very high and only trends are of interest (but not the absolute value). For example, even though the series by Varshneya et al. [16] seems to have a systematic error at high temperatures, its precision for soda-lime container and float glasses is superior to any other data published in the literature. Therefore, the trends of compositional changes on the electrical resistivity of soda-lime container and float glass melts can be determined with exceptional accuracy using models in ref. [5]. However, for estimating the accurate absolute value *and* accurate trends, models in this work are recommended.

Effects of glass components on the high-temperature electrical resistivity

The models in this study were developed in the way that the coefficients in Table IV directly reflect the resistivity change caused through an exchange of silica by 1 mol% of the considered glass component. For example if 1 mol% Li₂O is introduced into a silicate glass in exchange for silica, the decadic logarithm of the electrical resistivity (Ω·cm) would decrease 0.096 at 1000°C, 0.09 at 1200°C, and 0.074 at 1400°C, plus further changes due to component interactions. The

model intercepts in Table IV theoretically are supposed to represent the electrical resistivity of the residual comprising mainly SiO₂ and all insignificant [26] components. However, few experimental data exist for high-silica glasses, and the models in this paper are not applicable in those composition areas.

All glasses in this work contain SiO₂ as major component. Accordingly, all compositional influences summarized below represent interactions with SiO₂.

If a coefficient in Table IV is zero, it does not mean that the corresponding glass component is entirely unimportant. It only can be concluded that within the considered composition area, the component has no influence on the electrical resistivity.

For an accurate interpretation of model coefficients, the correlation matrices [26] given in ref. [38] must be considered. Unfortunately, none of the variables are absolutely statistically independent, i.e., all variables interfere mutually. It is believed that in the near future, it will be hardly possible to de-correlate all variables completely because it would require a high number of well-planned and very accurate measurements. Therefore, it is recommended to consider the model coefficients in this paper as preliminary findings until further experimental data become available. Nevertheless, as long as all concentration limits summarized in ref. [38] are followed, accurate predictions are possible.

Because of mutual correlations, it is suggested to compare model predictions rather than coefficient values for evaluating the influences of various glass components on the high-temperature electrical resistivity for a specific practical application. Examples are demonstrated in Figures 4 and 5.

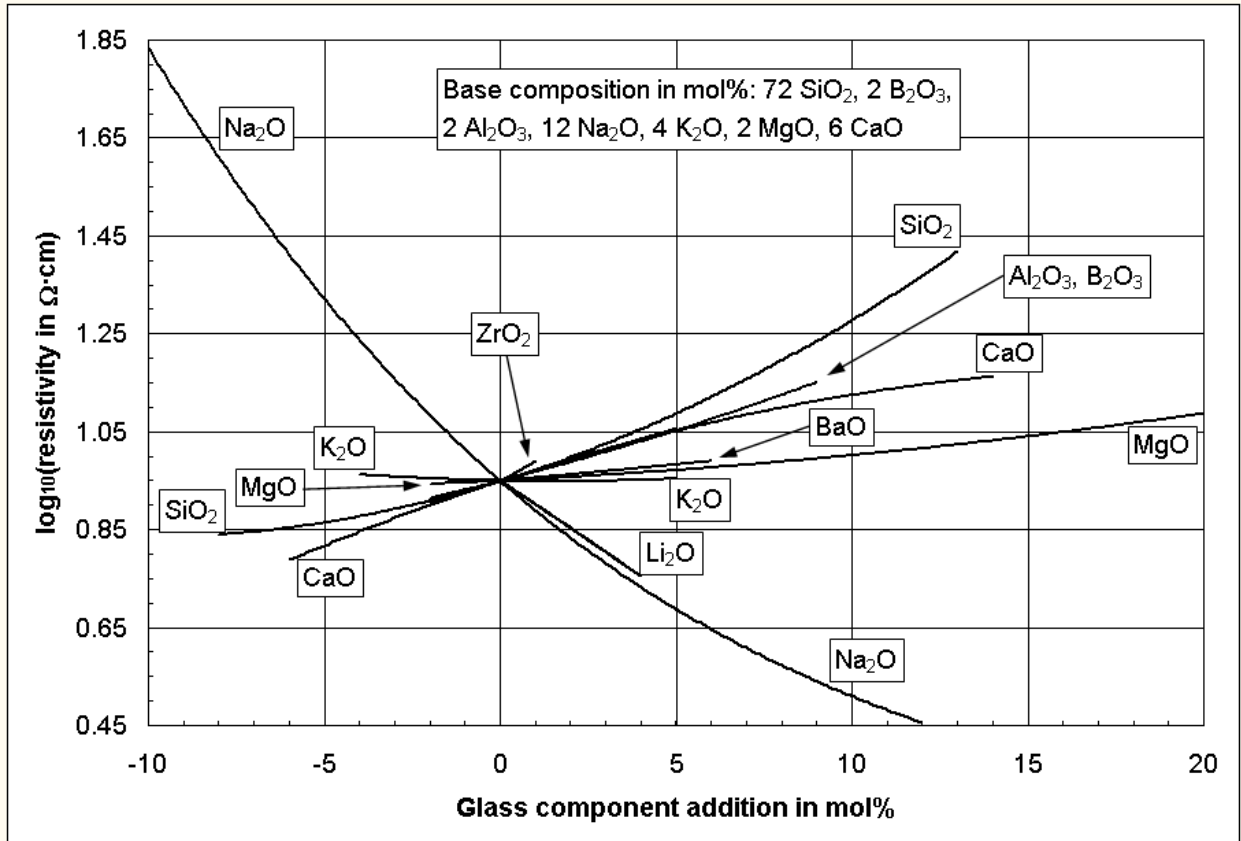


Figure 4: Spider-graph for specific base composition using the model at 1200°C; The spider-graph is different for other base compositions. For any component addition the ratios of all the remaining components stay constant.

Single-component influences

Glass former (SiO_2 , B_2O_3 , F)

SiO_2 (silica)

The influence of silica on the high-temperature electrical resistivity in this work is the difference resulting from the influences of the remaining glass components. In general, silica increases the high-temperature electrical resistivity significantly. Specific values can be derived from the models in Table IV or Figure 4.

B_2O_3 (boron oxide)

If silica is exchanged for boron oxide on a molar basis, it moderately influences the high-temperature electrical resistivity. This behavior could be expected because boron oxide does not add additional mobile ions to the glass that can transport electric current. Various boron oxide interactions may modify the B_2O_3 influence.

F (fluoride ions)

Based on the given data in the literature, fluoride ions have an insignificant influence on the high-temperature electrical resistivity, despite a strong decrease of the viscosity [5]. It is assumed that the fluoride ions partially "break" the silica glass-forming molecular network by forming terminal (non-bridging) Si-F bonds (i.e., the viscosity decreases); however, at the same time, the fluoride ions impede the movement of electrically conducting alkali ions through electrostatic

interaction. Fluoride ions seem to show a large discrepancy between the influence on the high-temperature electrical resistivity and the viscosity. Further investigations are desirable because no research is known to the authors where the influence of fluoride ions on the high-temperature electrical resistivity was systematically measured for commercial glasses.

Intermediate glass oxides (Al_2O_3 , ZrO_2 , Fe_2O_3)

Al_2O_3 (alumina)

Alumina increases the high-temperature electrical resistivity on its own, but many alumina interactions have the opposite effect (see below). The overall influence of alumina on the high-temperature electrical resistivity of multi-component glasses considering all component interactions largely depends on the chemical composition.

ZrO_2 (zirconium oxide)

Zirconium oxide increases the high-temperature electrical resistivity, particularly at low temperatures, probably based on its very strong influence on the viscosity [5, 39].

Fe_2O_3 (iron oxide)

For iron oxide, model coefficients are difficult to estimate because of its variable oxidation states, +2 (FeO) and +3 (Fe_2O_3). Oxidizing furnace atmospheres increase the Fe_2O_3 / FeO ratio, and reducing atmospheres decrease it. The reader is referred to studies where relatively high iron oxide concentrations were analyzed [3, 4]. In this work a significant influence of iron oxide on the high-temperature electrical resistivity was not observed.

Glass modifying oxides (Na_2O , K_2O , Li_2O , CaO , MgO , BaO , SrO , PbO , ZnO , water)

Na_2O (sodium oxide)

Sodium oxide strongly decreases the high-temperature electrical resistivity. For most common technical glass compositions it is the component that influences the electrical resistivity the most because of its high concentration.

K_2O (potassium oxide)

References [11, 14] and the mean orientation values in Tables I (system SiO_2 - Na_2O) and II (system SiO_2 - K_2O) make it evident that K_2O significantly decreases the high-temperature electrical resistivity as long as Na_2O or Li_2O are *not* present. In the presence of Na_2O or Li_2O , however, an increase in electrical resistivity resulting from the mixed-alkali effect (see below) may counteract or even reverse the decrease (see Figures 4 and 5).

Li_2O (lithium oxide)

Lithium oxide has a strong reducing effect on the high-temperature electrical resistivity on its own, but similar to potassium oxide, the mixed alkali effect and other interactions (see below) can counteract or reverse this influence, depending on the glass composition.

Alkaline earth oxides: MgO (magnesium oxide), CaO (calcium oxide, lime calcinated), SrO (strontium oxide), BaO (barium oxide)

Mazurina [17] observed for the first time that alkaline earth oxides increase the high-temperature electrical resistivity at lower temperatures, and they decrease it at higher temperatures. The light oxides MgO and CaO increase the resistivity less / decrease it more than the heavy oxides SrO and BaO , corresponding to their ionic sizes.

PbO (lead oxide)

Lead oxide shows a similar resistivity influence to alkali earth oxides. It must be noted that lead oxide has very different effects on other glass properties, for example viscosity [5, 39] or density and thermal expansion [40]; i.e., the other properties may be changed strongly without much influence on the high-temperature electrical resistivity.

ZnO (zinc oxide)

Zinc oxide moderately decreases the high-temperature electrical resistivity.

Water

The water concentrations of all transparent glasses in the study by Varshneya et al. [16, Appendix I at the end of the monograph, Tables I to VI] were analyzed by infrared spectroscopy. The concentrations varied from 80 to 640 ppm by weight (wt ppm), with an average of 280 wt ppm. No influence of water on the high-temperature electrical resistivity could be detected, probably due to its low concentration and data scattering. It is known from the literature, however, that water decreases the viscosity significantly at higher concentrations [41, 42, 43], which could have a similar effect on the electrical resistivity.

Component interactions

It is interesting to note that in most cases, the influence of component interactions decrease with increasing temperature, i.e., the interaction coefficients in Table IV decrease with increasing temperature. This effect might be caused by the increased dissociation of ionic associates as the glass melt temperature increases.

*Mixed alkali effects (Li_2O*Na_2O , Li_2O*K_2O , Na_2O*K_2O)*

If more than one alkali oxide is present in a glass melt, the alkali oxides interact in such a way that the electrical resistivity increases significantly [11, 14, 21, 24, 44, 45] where the Li_2O*K_2O and Na_2O*K_2O interactions have the strongest influence. The mixed alkali effect decreases with increasing temperature, but it practically never disappears, even at high melting temperatures. The coefficients in Table IV reflect this behavior well. According to Tickle [11], the Li_2O*K_2O mixed alkali effect is stronger than Na_2O*K_2O and Li_2O*Na_2O . In this paper, the Li_2O*K_2O interaction coefficient is slightly lower, however, than the Na_2O*K_2O interaction coefficient. This might be caused by the very few available experimental data of glasses containing high concentrations of Li_2O and K_2O simultaneously. To the authors' knowledge, only Tickle [11] (data in Table IX) and Kostanyan et al. [24] (data in Table XI) investigated the Li_2O*K_2O mixed-alkali effect, and their combined findings resulted in the Li_2O*K_2O coefficients in Table IV. Future experiments may lead to a clarification about the Li_2O*K_2O mixed-alkali effect, compared to the Na_2O*K_2O mixed-alkali effect.

For practical application, it is most beneficial to pay attention to the model predictions rather than the coefficients in Table IV because of mutual correlations. In addition, it is difficult to obtain a good overview of the electrical resistivity behavior in a specific system of interest, based on the interplay of numerous coefficients in Table IV. A graphical representation of model predictions can be helpful. An example is demonstrated in Figure 5. Figure 5 shows the contours of constant electrical resistivity at 1000°C for a soda-lime glass with the following composition in mol%: SiO_2 72.5, Al_2O_3 1.0, MgO 3.4, CaO 9.6, $Li_2O+Na_2O+K_2O$ 13.5. Figure 5 can be calculated using the coefficients in Table IV or ref. [38]. It is shown that in a soda-lime glass of the considered composition, Na_2O may be replaced through Li_2O on the molar basis without much influence on the electrical resistivity, as long as K_2O is low. This effect enables the

modification of the glass melt viscosity [5, 39], density and thermal expansion [40] without changing the electrical resistivity. The relations would be different on the basis of percent by weight (wt%). The maximum electrical resistivity is not obtained at $\text{Na}_2\text{O} / \text{K}_2\text{O} = 1$ as expected from mixed-alkali related publications, but at higher K_2O concentrations caused through various interactions of Na_2O and K_2O with CaO , MgO , and Al_2O_3 (Table IV). There exists an area on the K_2O -rich side of the diagram where compositional changes have little effect on the electrical resistivity. The contours of constant electrical resistivity in Figure 5 have a 95% confidence interval for multiple samples (simultaneous confidence interval) of about $\log_{10}(\rho/\Omega\cdot\text{cm}) = 0.05\text{-}0.2$, depending on the glass composition, the glass composition uncertainty not considered [38]. Since no experimental data exist so far, the diagram in Figure 5 can not fully be extended to the Li_2O -rich side ($\text{Li}_2\text{O} = 13.5$ mol%).

At a low temperature of 150°C Mazurin and Borisovskii found a ternary mixed-alkali effect in $\text{Li}_2\text{O}\text{-Na}_2\text{O}\text{-K}_2\text{O}\text{-SiO}_2$ glasses [46]. Such a ternary effect could not be detected in this work, probably because mixed-alkali effects decrease with increasing temperature.

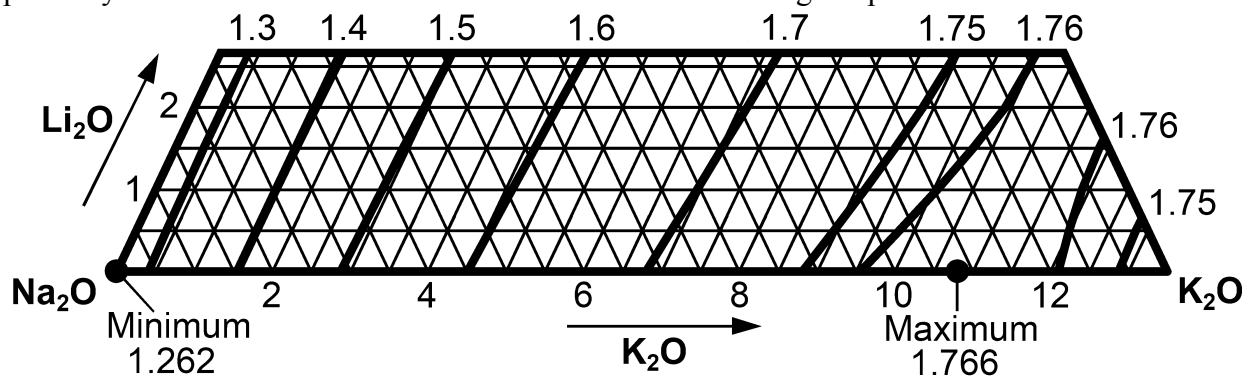


Figure 5: Contours of constant electrical resistivity at 1000°C for a soda-lime glass (concentrations in mol%: SiO_2 72.5, Al_2O_3 1.0, MgO 3.4, CaO 9.6, $\text{Li}_2\text{O}+\text{Na}_2\text{O}+\text{K}_2\text{O}$ 13.5); all concentrations in mol%; all electrical resistivity values in $\log_{10}(\rho/\Omega\cdot\text{cm})$; 95% confidence interval of electrical resistivity values for multiple samples in mass production (simultaneous confidence interval) ~ 0.05 to 0.2 (depending on glass composition, glass composition uncertainty not considered, see [38])

Reduction of non-bridging oxygen sites by alumina ($\text{Al}_2\text{O}_3*\text{Li}_2\text{O}$, $\text{Al}_2\text{O}_3*\text{Na}_2\text{O}$, $\text{Al}_2\text{O}_3*\text{K}_2\text{O}$)

It was observed by Isard [47] that alumina in four-fold coordination reduces the number of non-bridging oxygen sites in glass, which makes alkali ions more mobile and decreases the electrical resistivity. The coefficients in Table IV show the same trends.

Alkali – alkaline earth interactions ($\text{Li}_2\text{O}*\text{CaO}$, $\text{Na}_2\text{O}*\text{MgO}$, $\text{Na}_2\text{O}*\text{CaO}$, $\text{K}_2\text{O}*\text{CaO}$)

In the paper by Mazurin and Prokhorenko [2], it is concluded from model calculations that the interaction of (sum of $\text{Na}_2\text{O} + \text{K}_2\text{O}$) with (sum of $\text{MgO} + \text{CaO}$) increases the electrical resistivity of soda-lime glass at 1300°C , but it decreases it at 900°C and 600°C . In this work, the situation is more complex because several interactions are considered independently. It can be stated that the $\text{Na}_2\text{O}*\text{CaO}$ interaction is the most important one as Na_2O and CaO are present in many glasses in high concentrations. The $\text{Na}_2\text{O}*\text{CaO}$ interaction in this study follows a similar trend as observed by Mazurin and Prokhorenko. Other alkali – alkaline earth interactions follow various trends, but it may appear that with increasing molecular weight of the interacting oxides, the electrical resistivity increases, i.e., Li_2O and MgO interactions have a negative influence, but K_2O interactions have a positive influence. Always, a trend from negative to positive coefficients

occurs with increasing temperature. However, it is strongly advised at this point to consider the preliminary character of all coefficients due to the correlation interferences in Table II. The analysis of future experiments is required.

Boron oxide – modifier oxide interactions ($B_2O_3 \cdot K_2O$, $B_2O_3 \cdot MgO$)

As boron ions in glass vary their oxygen coordination number from three to four upon the introduction of alkali or alkaline earth oxides, it appears that this behavior increases the electrical resistivity through electrostatic interactions between boron and modifier ions. With increasing temperature, this effect decreases. Further experiments are desirable to clearly identify all interactions of boron oxide with Li_2O , Na_2O , and K_2O .

Boron oxide – alumina interaction ($B_2O_3 \cdot Al_2O_3$)

To the authors' knowledge, the influence of the interaction between boron oxide and alumina on the electrical resistivity of glass melts has never been investigated. It may be possible that both oxides pair in such a way in glass melts that the number of non-bridging oxygen sites is reduced significantly, but at the same time, alumina may "shield" boron so that it does not interact strongly with mobile modifying oxides. However, such statements remain speculation until further experimental data become available.

Sodium oxide – potassium oxide – calcium oxide ternary interaction ($Na_2O \cdot K_2O \cdot CaO$)

The $Na_2O \cdot K_2O \cdot CaO$ ternary interaction is required for successful modeling, especially at $1000^\circ C$. It may be assumed that the effect is real because of the numerous glasses that contain those three components at the same time and because the $Na_2O \cdot K_2O \cdot CaO$ interaction is only slightly correlated with the $Na_2O \cdot K_2O$ mixed alkali effect (Pearson's "r" = +0.3). It is too early at this point for further interpretations.

Recommendations for practical model application

The model in this paper is applicable to most commercial glass compositions. Although a few glasses for nuclear waste immobilization were included in the model development, the specialized models by Hrma et al. and Vienna et al. [3, 5] are recommended for these glasses (see also waste glass model in ref. [5]).

If electrical resistivity models are used for furnace design and operation assisted by mathematical modeling, several phenomena need to be considered: evaporation losses during the glass batch melting, possible influences of the oxidation states of transition metal oxides, electrode polarization effects, and the influence of potential gradients.

It is strongly advised to use the electrical resistivity calculator based on this study [38] because the appropriate concentration and component combination limits [26] of the models are evaluated automatically, and at the same time resistivity predictions, prediction confidence intervals, and the Vogel-Fulcher-Tammann constants of the resistivity-temperature curve are calculated. The resistivity calculator also considers glass-composition uncertainties in the error calculation, and it performs conversions from mol% to wt% and vice versa.

Need for standardized high-accuracy procedure and reference material

A general caution is required because according to Baucke [10] and Schiefelbein [9] electrical resistivity measurements of glass melts are not yet well established in scientific research. Scattering of the published experimental data and systematic errors occur and were detected during the modeling studies in this work. Even though it was attempted to correct systematic errors mathematically, it can not be ruled out completely that some systematic errors went

unnoticed leading to incorrect prediction errors. In the future, it would be beneficial to create a standardized procedure for measuring the electrical resistivity of glass melts with high accuracy. The procedure described by Schiefelbein et al. [9] appears most promising.

The creation of a standard reference material for high-temperature electrical resistivity of glass would be a tremendous help for calibration in various laboratories that are involved in resistivity measurements.

Conclusions

Models based on multiple regression using polynomial functions were provided for estimating the high-temperature electrical resistivity of silicate glasses from their chemical composition with high accuracy. The influences of specific glass components and component interactions could be quantified. Some important glass components are not included as yet. A number of interactions are correlated too strongly for analysis within the composition region covered. Notwithstanding these shortcomings, success in the estimation of the electrical resistivity from the chemical composition has been demonstrated.

It was suggested that a standard procedure similar to Schiefelbein et al. [9] for measuring the electrical resistivity of glass melts should be established in the future, and a standard reference glass should be created.

Acknowledgments

The authors would like to extend a special thanks to Oleg V. Mazurin (St. Petersburg, Russia), Pavel Hрма (Pacific Northwest National Laboratory, Richland, Washington, USA), Ralf Keding (Institute of Glass Chemistry, Jena, Germany), Christian Rüssel (Institute of Glass Chemistry, Jena, Germany), Henry Foxhall (Glass Technology Services, Sheffield, Great Britain), Robert Williams (Alfred University, Alfred, New York, USA), and Harold S. Haller (Case Western Reserve University, Cleveland, Ohio, USA) for very valuable comments and discussions. Terese Vascott, Ramesh Karuppanan, and Jeffrey M. Jones performed a large number of measurements summarized by Varshneya et al. [16]. The authors also thank the Center for Environmental and Energy Research at Alfred University (supported by the U.S. Environmental Protection Agency), the National Science Foundation Industry/University Center for Glass Research, and the U.S. Department of Energy (Grant DE FG 07-96EE41262) for funding the modeling and outreach efforts.

Appendix (A), model source data

Appendix (B) summarizes the references and modeling results in the three systems $\text{SiO}_2\text{-Na}_2\text{O}$, $\text{SiO}_2\text{-K}_2\text{O}$, and $\text{SiO}_2\text{-CaO-Na}_2\text{O}$. In addition, data from the following publications were included in the models: Mazurin et al. [2], Tickle [11], Kim et al. [14], retracted NIST standard SRM 1414 [15], Varshneya et al. [16], Mazurina et al. [17], Baucke et al. [21], Pfeiffer [22], Vienna et al. [3], Kirakosyan et al. [23], Kostanyan et al. [24].

The tables below list all source data, except Varshneya et al. [16], Mazurin et al. [2], Vienna et al. [3] (data also summarized in reference [5]), retracted NIST standard SRM 1414 [15], and the mean orientation values in the three systems $\text{SiO}_2\text{-Na}_2\text{O}$, $\text{SiO}_2\text{-K}_2\text{O}$, and $\text{SiO}_2\text{-CaO-Na}_2\text{O}$ (see Appendix (B)).

The experimental findings by Saringyulyan et al. [28], which are *not* considered in the models of this study, are given in Table XVI to estimate lead glass resistivities.

Table VIII: Data-series by Baucke et al. [21]

Glass composition in mol%				$\log_{10}(\rho/\Omega\cdot\text{cm})$		
SiO ₂	CaO	Na ₂ O	K ₂ O	1000°C	1200°C	1400°C
73.70	10.80	15.50	0.00	1.12	0.77	0.54
73.70	10.80	13.56	1.94	1.25	0.86	0.61
73.70	10.80	11.63	3.87	1.38	0.96	0.69
73.70	10.80	9.69	5.81	1.50	1.04	0.74
73.70	10.80	7.74	7.75	1.58	1.09	0.79
73.70	10.80	5.81	9.68	1.63	1.14	0.82
73.70	10.80	3.87	11.62	1.62	1.13	0.81
73.70	10.80	1.94	13.55	1.58	1.11	0.80
73.70	10.80	0.00	15.49	1.51	1.06	0.78

Table IX: Data-series by Tickle [11], outlier in parenthesis / not listed

Glass composition in mol%				$\log_{10}(\rho/\Omega\cdot\text{cm})$		
SiO ₂	Li ₂ O	Na ₂ O	K ₂ O	1000°C	1200°C	1400°C
80.0	5.0	15.0	0.0	0.88	0.58	0.40
80.0	10.0	10.0	0.0	0.85	0.56	0.36
80.0	15.0	5.0	0.0	0.78	0.55	0.36
80.0	5.0	0.0	15.0	1.26	0.87	0.61
80.0	10.0	0.0	10.0	1.60	(1.16)	0.82
80.0	15.0	0.0	5.0	1.33	0.94	0.68
70.3	0.0	29.7	0.0	0.20	-0.02	-0.16
65.3	0.0	34.7	0.0	0.00	-0.20	-0.33
60.5	0.0	39.5	0.0	-0.13	-0.32	-0.45

Table X: Data-series by Kim et al. [14], outliers in parenthesis / not listed

Glass composition in mol%				$\log_{10}(\rho/\Omega\cdot\text{cm})$		
SiO ₂	Al ₂ O ₃	Na ₂ O	K ₂ O	1000°C	1200°C	1400°C
75.00	0.00	25.00	0.00	0.45	0.28	0.19
75.00	0.00	18.75	6.25	(0.59)	0.39	0.26
75.00	0.00	12.50	12.50	(0.69)	0.47	0.31
75.00	0.00	6.25	18.75	0.71	0.48	0.31
75.00	0.00	0.00	25.00	0.63	0.40	0.28
70.00	5.00	25.00	0.00	0.49	0.32	0.23
70.00	5.00	18.75	6.25	0.72	0.47	0.32
70.00	5.00	12.50	12.50	0.86	0.58	0.41
70.00	5.00	6.25	18.75	0.88	0.59	0.42
70.00	5.00	0.00	25.00	0.76	0.49	0.33
67.50	7.50	25.00	0.00	0.54	(0.36)	0.25
67.50	7.50	18.75	6.25	0.80	0.53	0.38
67.50	7.50	12.50	12.50	1.02	0.67	0.49
67.50	7.50	6.25	18.75	1.05	0.69	0.51
67.50	7.50	0.00	25.00	0.86	0.56	0.39
65.00	10.00	18.75	6.25	0.87	0.59	0.44
65.00	10.00	12.50	12.50	1.17	0.77	0.57
65.00	10.00	0.00	25.00	0.97	0.63	0.45

Table XI: Data-series by Kostanyan et al. [24]

Glass composition in mol%				$\log_{10}(\rho/\Omega\cdot\text{cm})$		
SiO ₂	Li ₂ O	Na ₂ O	K ₂ O	1000°C	1200°C	1400°C
75.0	17.5	7.5	0.0	0.536	0.268	0.105
75.0	12.5	12.5	0.0	0.631	0.349	0.193
75.0	7.5	17.5	0.0	0.550	0.290	0.150
75.0	17.5	0.0	7.5	1.010	0.690	0.480
75.0	12.5	0.0	12.5	1.200	0.840	0.610
75.0	7.5	0.0	17.5	1.100	0.760	0.570

Table XII: Data-series by Mazurina et al. [17], outliers in parenthesis

Glass composition in mol%							$\log_{10}(\rho/\Omega\cdot\text{cm})$		
SiO ₂	Na ₂ O	K ₂ O	MgO	CaO	SrO	ZnO	1000°C	1200°C	1400°C
80	15	0	5	0	0	0	1.05	0.77	0.56
75	15	0	10	0	0	0	0.93	0.62	0.41
70	15	0	15	0	0	0	0.87	0.55	0.32
65	15	0	20	0	0	0	0.83	0.51	0.29
60	15	0	25	0	0	0	0.87	0.48	0.23
80	15	0	0	5	0	0	1.02	0.70	0.52
75	15	0	0	10	0	0	0.97	0.65	0.43
70	15	0	0	15	0	0	(0.98)	0.61	0.36
65	15	0	0	20	0	0	1.15	0.70	0.42
60	15	0	0	25	0	0	1.25	0.66	0.34
75	15	0	0	0	0	10	0.77	0.44	0.24
70	15	0	0	0	0	15	0.77	0.44	0.24
65	15	0	0	0	0	20	0.83	0.50	0.28
60	15	0	0	0	0	25	0.82	0.40	0.18
75	15	0	0	0	10	0	1.22	0.85	0.59
70	15	0	0	0	15	0	1.19	0.78	0.48
65	15	0	0	0	20	0	1.32	0.76	0.42
80	0	15	5	0	0	0	1.31	0.93	0.67
75	0	15	10	0	0	0	(1.59)	1.16	0.87
70	0	15	15	0	0	0	1.43	0.99	0.69
65	0	15	20	0	0	0	1.57	1.11	0.80
60	0	15	25	0	0	0	1.58	1.09	0.79
55	0	15	30	0	0	0	1.60	1.11	0.78
80	0	15	0	5	0	0	1.37	0.94	(0.68)
75	0	15	0	10	0	0	1.66	1.23	0.91
70	0	15	0	15	0	0	1.86	1.34	0.97
65	0	15	0	20	0	0	1.80	1.23	0.83
60	0	15	0	25	0	0	1.96	1.32	0.91
55	0	15	0	30	0	0	2.10	1.39	0.89

Table XIII: Data-series by Kirakosyan et al. [23], outlier in parenthesis

Glass composition in mol%			$\log_{10}(\rho/\Omega\cdot\text{cm})$		
SiO ₂	Al ₂ O ₃	Na ₂ O	1000°C	1200°C	1400°C
80	0	20	0.72	0.38	0.16
70	10	20	(0.98)	0.53	0.32
64	16	20	0.79	0.56	0.32
60	20	20	0.74	0.52	0.32
58	22	20	0.77	0.56	0.32
56	24	20	0.84	0.58	0.32

Table XIV: Data-series by Pfeiffer [22], outlier in parenthesis

Glass composition in mol%							$\log_{10}(\rho/\Omega\cdot\text{cm})$		
SiO ₂	B ₂ O ₃	Al ₂ O ₃	Na ₂ O	K ₂ O	CaO	BaO	1000°C	1200°C	1400°C
70.0	0.0	0.8	12.0	2.0	7.0	7.5	(1.306)	0.906	0.653
83.0	11.0	1.5	3.5	0.5	0.0	0.0	2.319	1.916	(1.647)
78.0	9.0	3.0	6.5	0.3	1.5	1.0	1.845	1.474	1.218

Table XV: Electrical resistivity measurement frequencies

Baucke et al. [21]	0.1-100 kHz
Tickle [11]	1-10 kHz
Varshneya et al. [16]	2 kHz
Mazurin et al. [2]	> 1 kHz
Kim et al. [14]	4 kHz
Vienna et al. [3]	0.1-100 kHz
Kostanyan et al. [24]	50 Hz
Mazurina et al. [17]	unknown
Kirakosyan et al. [23]	unknown
Pfeiffer [22]	0.1-100 kHz
NIST standard SRM 1414 [15], retracted	~1-10 kHz
SiO ₂ -Na ₂ O, SiO ₂ -K ₂ O, and SiO ₂ -CaO-Na ₂ O	variable

Table XVI: Data-series by Saringyulyan [28] (lead glasses by Saringyulyan *not* included in this work because of the unique glass compositions studied), determination of electrical resistivity by direct measurements of current and voltage using graphite paint electrodes, and by AC bridge method using alumina crucible and platinum wire electrodes, frequency 800 Hz [25]; the slash "/" stands for not measured

Glass composition in mol%			$\log_{10}(\rho/\Omega\cdot\text{cm})$ at T in °C											
SiO ₂	PbO	K ₂ O	300	400	500	600	700	800	900	1000	1100	1200	1300	1400
80	0	20	5.12	4.06	3.08	2.29	/	1.36	/	0.82	0.62	0.48	0.35	0.23
70	10	20	/	4.73	/	2.43	/	1.43	/	0.90	0.68	0.49	0.34	0.20
60	20	20	/	/	/	2.39	/	1.32	/	0.77	0.56	0.36	0.20	0.06
50	30	20	/	4.97	/	2.31	/	1.16	/	0.59	0.37	0.19	0.03	/
80	10	10	/	6.73	/	4.34	/	2.92	/	2.17	1.88	1.63	1.42	1.22
70	20	10	/	/	/	4.26	/	2.74	/	1.94	1.64	1.38	1.15	0.95
60	30	10	/	/	/	4.19	/	2.42	/	1.51	1.22	0.97	0.76	0.58
50	40	10	/	6.82	/	3.40	/	1.70	/	0.96	0.70	0.49	0.30	/
70	0	30	/	3.19	/	1.69	/	0.84	/	0.43	0.26	0.13	0.00	-0.11
60	10	30	/	3.45	/	1.60	/	0.77	/	0.34	0.16	0.02	/	/
70	30	0	/	/	/	5.23	/	3.13	/	2.12	1.77	1.49	1.24	1.02
60	40	0	/	/	/	5.46	/	3.00	/	1.76	1.43	1.16	0.92	0.72
50	50	0	/	7.45	/	4.04	/	2.02	/	1.07	0.79	0.55	0.34	/
40	40	20	6.81	5.40	4.36	3.54	1.48	1.08	0.77	0.54	0.32	0.14	/	/
60	0	40	3.36	2.52	1.92	1.28	0.78	0.47	0.25	0.07	-0.10	/	/	/
40	50	10	/	/	4.30	2.32	1.65	1.14	0.77	0.50	/	/	/	/
50	20	30	/	3.44	2.26	1.44	0.99	0.66	0.42	0.21	0.03	/	/	/
77	5	18	5.72	4.58	3.47	2.67	2.09	1.64	1.30	1.02	0.83	0.67	0.53	0.42
70	16.7	13.3	/	6.91	5.32	4.10	3.2	2.59	2.14	1.76	1.46	1.24	1.04	0.87
66.5	22.5	11	/	/	5.85	4.60	3.64	2.90	2.35	1.91	1.60	1.35	1.12	0.93
65	25	10	/	/	6.03	4.75	3.76	2.95	2.18	1.94	1.58	1.33	1.10	0.90
63.5	27.5	9	/	/	7.47	5.05	3.92	3.08	2.45	1.95	1.59	1.33	1.10	0.90
61.5	30.8	7.7	/	8.07	6.40	4.89	3.72	2.87	2.22	1.72	1.38	1.13	0.91	0.71
60	33.3	6.7	/	/	6.50	5.00	3.82	2.91	2.24	1.75	1.44	1.17	0.94	0.73
57.5	37.5	5	/	8.10	6.40	4.83	3.51	2.63	1.96	1.54	1.19	0.95	0.73	0.55
54.2	43	2.8	/	5.71	4.02	2.74	1.91	1.34	0.98	0.69	0.44	0.23	0.04	/
52.5	45.8	1.7	/	5.90	4.10	2.74	1.95	1.37	0.96	0.68	0.43	0.23	0.04	/

APPENDIX (B), Modeling procedure and references for establishing the mean orientation values in the systems SiO₂-Na₂O, SiO₂-K₂O, and SiO₂-CaO-Na₂O [5]

Because only a limited number of high-temperature electrical resistivity data exist in the scientific literature (e.g., compared to the viscosity), three simple glass forming systems were used as guide for comparison which were studied by many investigators: SiO₂-Na₂O, SiO₂-K₂O,

and SiO₂-CaO-Na₂O. All properties were obtained from SciGlass [25] and Mazurin et al. [2]. Detailed references are given below. It was assumed that the majority of the data in the literature are comparable, i.e., the investigators considered the electrical resistivity considering ionic and electrode polarization effects appropriately [2], as well as capacitive and inductive losses. The data of the analyzed systems were combined and grouped according to reference resistivities at 1000°C, 1200°C, and 1400°C. Three independent polynomial slack variable models (excluding silica, with intercept, see Equation (3)) were developed at 1000°C, 1200°C, and 1400°C from 110 to 160 data points at each of the three temperatures. The models were based on mol% including all linear variables Na₂O, K₂O, and CaO, and the following higher order terms: (Na₂O)², (Na₂O)³, (K₂O)², (K₂O)³, and the Na₂O*CaO interaction. The model standard errors were log($\rho/\Omega\cdot\text{cm}$) = 0.052 at 1000°C, 0.094 at 1200°C, and 0.105 at 1400°C. The regression R² were 0.986 at 1000°C, 0.946 at 1200°C, and 0.928 at 1400°C. Predictions of the three independent intermediate models at 1000°C, 1200°C, and 1400°C were combined by applying regression using a quadratic function, with the squared term set to a constant average value. The regression between the models resulted in an additional error of log($\rho/\Omega\cdot\text{cm}$) = 0.013. Tables I to III show the final mean orientation values and 95% confidence intervals for the mean resistivity with the concentrations in mol% and wt%. Detailed references are listed below, as given in SciGlass [25]:

System SiO₂-Na₂O:

- Ashizuka M., Ohtani M.; J. Jpn. Inst. Metals, 1969, vol. 33, No. 4, p 498.
- Bockris J. O'M., Kitchener J. A., Ignatowicz S., Tomlinson J. W., Trans. Faraday Soc., 1952, vol. 48, No. 1, p 75.
- Bonetti G., Lazzari S.; Vetro e Silicati, 1969, vol. 13, No. 5, p 5.
- Bonetti G.; Riv. Staz. Sper. Vetro, 1976, vol. 6, No. 6, p 241.
- Boricheva V. N.; Issledovanie Elektroprovodnosti Nekotorykh Prostykh Silikatnykh Stekol v Shirokom Intervale Temperatur, Thesis, Leningrad, 1956.
- Botvinkin O. K., Okhotin M. V.; in: Noveishie Raboty po Fizicheskoi Khimii Stekla, Moskva, 1936, p 72.
- Buchanan R. C., Kingery W. D.; Compt. Rend. VII Congr. Intern. du Verre, Bruxelles, 1965, vol. 2, p 368.
- Evstropiev K. S.; in: Fiziko-Khimicheskie Svoistva Troinoi Sistemy Na₂O-PbO-SiO₂, Moskva, 1949, p 83.
- Gukasyan S. B., Kostanyan K. A.; Dokl. Akad. Nauk Arm. SSR, 1978, vol. 67, No. 2, p 101.
- Kawahara M., Ozima Y., Morinaga K., Yanagase T.; J. Jpn. Inst. Metals, 1978, vol. 42, No. 6, p 618.
- Kostanyan K. A., Erznkyan E. A.; Dokl. Akad. Nauk Arm. SSR, 1966, vol. 43, No. 5, p 279.
- Kostanyan K. A., Kirakosyan S. Sh.; Arm. Khim. Zh., 1974, vol. 27, No. 7, p 547.
- Kostanyan K. A., Saakyan K. S.; Izv. Akad. Nauk Arm. SSR, Khim. Nauki, 1961, vol. 14, No. 5, p 409.
- Kostanyan K. A., Shakhmuradyan G. T.; Arm. Khim. Zh., 1975, vol. 28, No. 9, p 692.
- Kostanyan K. A., Erznkyan E. A., Avetisyan E. M.; Arm. Khim. Zh., 1967, vol. 20, No. 8, p 592.
- Kostanyan K. A., Erznkyan E. A., Loryan Yu. G.; in: Stekloobraznoe Sostoyanie, Erevan, 1970, p 206.
- Kostanyan K. A.; Fizika i Khimiya Stekla, 1982, vol. 8, No. 6, p 650.
- Kroger C., Weisgerber P.; Z. Phys. Chem., 1958, vol. 18, No. 1/2, p 90.
- Lotto B., Lazzari S.; Vetro e Silicati, 1965, vol. 9, No. 50, p 5.
- Mori K.; J. Iron Steel Inst. Jpn., 1956, vol. 42, No. 8, p 633.

- Morinaga K., Suginothara Y., Yanagase T.; J. Jpn. Inst. Metals, 1975, vol. 39, No. 12, p 1312.
- Piechurovski A.; 4^e Conference sur la fusion electrique du verre, Tchecoslovaque, 1972, vol. 2, p 16.
- Shakhmuradyan G. T., Kostanyan K. A., Dzhavuktsyan S. G. ; Arm. Khim. Zh., 1976, vol. 29, No. 3, p 218.
- Shinozaki N., Okusu H., Mizoguchi K., Suginothara Y. ; J. Jpn. Inst. Metals, 1977, vol. 41, No. 6, p 607.
- Stanek J., Sasek L., Meissnerova H.; Sprechsaal, 1966, No. 5, p 151.
- Urnes S.; Glass Industry, 1959, vol. 40, No. 5, p 237.
- Wakabayashi H., Terai R.; Bull. Governm. Ind. Res. Inst. Osaka, 1984, vol. 35, No. 1, p 58.
- Wakabayashi H., Terai R.; J. Ceram. Soc. Jpn., 1983, vol. 91, No. 7, p 334.
- Wakabayashi H., Terai R.; J. Ceram. Soc. Jpn., 1985, vol. 93, No. 1, p 13.
- References [11, 14, 23, 24]

Excluded from the calculation due to significant inconsistency with other investigators: Endell and Hellbrügge [30]

System SiO₂-K₂O:

- Ashizuka M.; J. Ceram. Soc. Jpn., 1989, vol. 97, No. 4, p 489.
- Bockris J. O'M., Kitchener J. A., Ignatowicz S., Tomlinson J. W.; Trans. Faraday Soc., 1952, vol. 48, No. 1, p 75.
- Boricheva V. N.; Issledovanie Elektroprovodnosti Nekotorykh Prostykh Silikatnykh Stekol v Shirokom Intervale Temperatur, Thesis, Leningrad, 1956.
- Kostanyan K. A., Erznkyan E. A.; Dokl. Akad. Nauk Arm. SSR, 1966, vol. 43, No. 5, p 279.
- Kostanyan K. A., Erznkyan E. A.; Izv. Akad. Nauk Arm. SSR, Khim. Nauki, 1964, vol. 17, No. 6, p 613.
- Kostanyan K. A., Saringyulyan R. S.; Elektrokhimiya i Rasplavy, Moskva, 1974, p 193.
- Kostanyan K. A., Shakhmuradyan G. T.; Arm. Khim. Zh., 1975, vol. 28, No. 9, p 692.
- Kostanyan K. A., Erznkyan E. A., Loryan Yu. G.; in: Stekloobraznoe Sostoyanie, Erevan, 1970, p 206.
- Sasek L., Meissnerova H., Persin J.; Sb. Vys. Sk. Chem. Technol. Praze, Chem. Technol. Silik., 1973, vol. L4, p 87.
- Urnes S.; Glass Industry, 1959, vol. 40, No. 5, p 237.
- Wakabayashi H., Terai R.; Bull. Governm. Ind. Res. Inst. Osaka, 1984, vol. 35, No. 1, p 58.
- Wakabayashi H., Terai R.; J. Ceram. Soc. Jpn; 1983, vol. 91, No. 7, p 334.
- References [11, 14, 17, 24, 28]

Excluded from the calculation due to significant inconsistency with other investigators: Endell and Hellbrügge [30]

System SiO₂-Na₂O-CaO:

- Bonetti G., Lazzari S.; Vetro e Silicati, 1969, vol. 13, No. 5, p 5.
- Bonetti G.; Riv. Staz. Sper. Vetro, 1976, vol. 6, No. 6, p 241.
- Boricheva V. N.; Issledovanie Elektroprovodnosti Nekotorykh Prostykh Silikatnykh Stekol v Shirokom Intervale Temperatur, Thesis, Leningrad, 1956.
- Botvinkin O. K., Okhotin M. V.; in: Noveishie Raboty po Fizicheskoi Khimii Stekla, Moskva, 1936, p 72.
- Kostanyan K. A., Geokchyan O. K.; Steklo Keram., 1964, No. 4, p 5.
- Kostanyan K. A.; Issledovanie Elektroprovodnosti Natrii-Kaltsii-Magnii-Alyumosilikatnykh Stekol v Rasplavlennom Sostoyanii, Thesis, Leningrad, 1952.

- Kostanyan K. A., Saakyan K. S., Geokchyan O. K.; *Izv. Akad. Nauk Arm. SSR, Khim. Nauki*, 1964, vol. 17, No. 4, p 357.
- Kroger K., Heckmann H.; *Glastechn. Ber.*, 1966, vol. 39, No. 11, p 479.
- Mazurin O. V.; *Tr. Leningr. Tekhnol. Inst.*, 1954, No. 29, p 72.
- Mazurina E. K., Evstropiev K. S.; *Izv. Vyssh. Uchebn. Zaved., Khimiya i Khim. Tekhnol.*, 1967, No. 6, p 673.
- Stanek J., Sasek L., Meissnerova H.; *Sprechsaal*, 1966, No. 5, p 151.
- Wakabayashi H., Terai R.; *Bull. Governm. Ind. Res. Inst. Osaka*, 1984, vol. 35, No. 1, p 58.
- Wakabayashi H., Terai R.; *J. Ceram. Soc. Jpn*, 1983, vol. 91, No. 7, p 334.
- References [2, 17]

References

- [1] J. Stanek: "Electric Melting of Glass"; Elsevier Scientific Publishing, Amsterdam 1977.
- [2] O. V. Mazurin, O. A. Prokhorenko: "Electrical conductivity of glass melts"; Chapter 10 in: "Properties of Glass-Forming Melts" ed. by D. L. Pye, I. Joseph, A. Montenaro; CRC Press, Boca Raton, Florida, 2005, ISBN 1-57444-662-2.
- [3] J. D. Vienna, P. R. Hrma et al.: "Effect of Composition and Temperature on the Properties of High Level Waste (HLW) Glass Melting above 1200°C (Draft)"; PNNL Report 10987 to the US Department of Energy, Contract DE-AC06-76RLO 1830, February 1996.
<http://www.osti.gov/dublincore/gpo/servlets/purl/212394-mv0A6T/webviewable/>
Data also summarized in reference [5]
- [4] P. Hrma, R. J. Robertus: "Waste glass design based on property composition functions"; Ceram. Eng. Sci. Proc., vol. 14, 1993, no. 11/12, p 187-203.
P. Hrma, G. F. Piepel, P. E. Redgate, D. E. Smith, M. J. Schweiger, J. D. Vienna, D. S. Kim: "Prediction of processing properties for nuclear waste glasses"; Ceramic Transactions, vol. 61, p 505-513.
P. R. Hrma, G. F. Piepel et al.: "Property/Composition Relationships for Hanford High-Level Waste Glasses Melting at 1150°C"; PNL Report 10359 to the US Department of Energy, vol. 1 and 2, Contract DE-AC06-76RLO 1830, December 1994.
<http://www.osti.gov/dublincore/gpo/servlets/purl/10121755-P8oQTI/webviewable/>
<http://www.osti.gov/dublincore/gpo/servlets/purl/10121752-cDjMo0/webviewable/>
- [5] A. Fluegel, D. A. Earl, A. K. Varshneya, D. Öksoy: "Statistical analysis of viscosity, electrical resistivity, and further glass melt properties", Chapter 9 in: "High temperature glass melt property database for process modeling"; Eds.: T. P. Seward III and T. Vascott; The American Ceramic Society, Westerville, Ohio, 2005, ISBN 1-57498-225-7.
- [6] C. J. Leo, B. V. R. Chowdari, G. V. Subba Rao, J. L. Souquet: "Lithium conducting glass ceramic with Nasicon structure"; Materials Research Bulletin, 2002, vol. 37, p 1419-1430.
[http://dx.doi.org/10.1016/S0025-5408\(02\)00793-6](http://dx.doi.org/10.1016/S0025-5408(02)00793-6)
- [7] Ch. Ravagnani, R. Keding, Ch. Rüssel: "High temperature impedance spectroscopy of homogeneous and phase separated melts and glasses of the composition 48.5 SiO₂ - 48.5 B₂O₃ - 3 Na₂O"; J. Non-Cryst. Solids, 2003, vol. 328, p 164-173.
[http://dx.doi.org/10.1016/S0022-3093\(03\)00475-7](http://dx.doi.org/10.1016/S0022-3093(03)00475-7)
- [8] R. Keding, D. Tauch, Ch. Rüssel: "Electrical impedance determination of phase transitions in glasses and melts"; J. Non-Cryst. Solids, 2004, vol. 348, p 123-130.
<http://dx.doi.org/10.1016/j.jnoncrysol.2004.08.137>
- [9] S. L. Schiefelbein, N. A. Fried, K. G. Rhoads, D. R. Sadoway: "A high-accuracy, calibration-free technique for measuring the electrical conductivity of liquids"; Review of Scientific Instruments, vol. 69, Sept 1998, no. 9, p 3308-3313.
<http://web.mit.edu/dsadoway/www/77.pdf>
S. L. Schiefelbein, D. R. Sadoway: "A high-accuracy, calibration-free technique for measuring the electrical conductivity of molten oxides"; Metallurgical and Materials Transactions B, vol. 28B, Dec 1997, p 1141-1149.
S. L. Schiefelbein; Ph.D. Thesis, Massachusetts Institute of Technology, Cambridge, MA, 1996.
- [10] F. G. K. Baucke, W. A. Frank: "Conductivity cell for molten glasses and salts"; Glastechn. Ber., vol 49, 1976, no. 7, p 157-161.

- F. G. K. Baucke, J. Braun: "Accurate conductivity cell for molten glasses and salts"; *Glastechn. Ber.*, vol. 62, 1989, no. 4, p 122-126.
- F. G. K. Baucke, K. Mücke: "Measurement of standard Seebeck coefficients in non-isothermal glass melts by means of ZrO₂ electrodes"; *J. Non-Cryst. Solids*, vol. 84, July 1986, p 174-182.
[http://dx.doi.org/10.1016/0022-3093\(86\)90775-1](http://dx.doi.org/10.1016/0022-3093(86)90775-1)
- [11] R. E. Tickle: "The electrical conductance of molten alkali silicates"; *Phys. Chem. Glasses*, vol. 8, 1967, no. 3, p 101-124.
- [12] Mach; *Silikaty*, vol. 4, 1960, p 357.
- [13] Yu. K. Startsev: "Technique for measuring the electric conductivity of glasses and melts over a wide temperature range covering the glass transition region"; *Glass Phys. Chem.*, vol. 26, 2000, no. 1, p 73-82.
- [14] K. D. Kim; *Proc. XVIIth Intern. Congr. on Glass, Beijing 1995*, vol. 3, p 747.
 K. D. Kim: "Resistivity measurement of molten glass and mixed alkali effect in sodium and potassium silicate melts"; *Glass Technol.* vol. 36, 1995, no. 1, p 27-31.
 K. D. Kim: "Electrical conductivity in mixed-alkali aluminosilicate melts"; *J. Am. Ceram. Soc.*, vol. 79, 1996, no. 9, p 2422-2428.
 K. D. Kim, and S.-H. Lee; *J. Ceram. Soc. Jpn*, vol. 105, 1997, no. 10, p 827.
- [15] Standard Reference Material (SRM) 1414 (Lead-Alkali Silicate Glass), Electrical Resistivity, National Institute of Standards and Technology (NIST), 1991 (Standard retracted by NIST).
- [16] K. Varshneya, T. Vascott: "Electrical resistivity", Chapter 8 in: "High temperature glass melt property database for process modeling"; Eds.: T. P. Seward III and T. Vascott; The American Ceramic Society, Westerville, Ohio, 2005, ISBN 1-57498-225-7.
- [17] E. K. Mazurina; *Steklo*, 1967, no. 1, p 129.
 E. K. Mazurina, K. S. Evstropiev, in: *Stekloobraznoe Sostoyanie*, Erevan, 1970, p 195.
 E. K. Mazurina: "Influence of two-valence metal oxides on electrical conductivity of alkali silicate glasses in the temperature range 200-1400°C (in Russian), Thesis, Lensoviet Technological Institute, Leningrad, 1967.
- [18] Ch. Rüssel: "Redox Behavior and Electrochemical Behavior of Glass Melts"; Chapter 3 in: "Properties of Glass-Forming Melts" ed. by D. L. Pye, I. Joseph, A. Montenegro; CRC Press, Boca Raton, Florida, 2005, ISBN 1-57444-662-2.
- [19] H. Schirmer, R. Keding, Ch. Rüssel: "Thermodynamics of the Sn²⁺/Sn⁴⁺ equilibrium in Li₂O/Al₂O₃/SiO₂ glass melts studied by square-wave voltammetry and impedance spectroscopy"; *J. Non-Cryst. Solids*, vol. 336, 2004, p 37-43.
<http://dx.doi.org/10.1016/j.jnoncrysol.2003.12.052>
- [20] D. Benne, R. Keding, Ch. Rüssel: "Redox equilibria in a tin doped melt with the basic composition 16 Li₂O, 10 CaO, 74 SiO₂ studied by square-wave voltammetry and impedance spectroscopy"; *Phys. Chem. Glasses*, vol. 45, 2004, p 45-51.
- [21] F. G. K. Baucke: "Mixed alkali effect of electrical conductivity in glass-forming silicate melts"; *Glastechn. Ber.*, vol. 62, 1989, no. 5, p 182-186.
 F. G. K. Baucke, R.-D. Werner; *Proc. XVth Intern. Congr. on Glass, Leningrad*, vol. 2, 1989, p 242.
- [22] T. Pfeiffer: "Viscosities and electrical conductivities of oxidic glass-forming melts"; *Solid State Ionics*, vol. 105, Jan 1998, p 277-287.
[http://dx.doi.org/10.1016/S0167-2738\(97\)00475-X](http://dx.doi.org/10.1016/S0167-2738(97)00475-X)

- [23] S. Sh. Kirakosyan; in: Stekloobraznoe Sostoyanie, Erevan, 1974, p 78.
K. A. Kostanyan, S. Sh. Kirakosyan; Arm. Khim. Zh., vol. 27, 1974, no. 7, p 547.
- [24] K. A. Kostanyan, E. A. Erznkyan; Arm. Khim. Zh., vol. 20, 1967, no. 9, p 686.
- [25] SciGlass 6.5 Database and Information System, 2005.
<http://www.sciglass.info/>
- [26] A. Fluegel: "Statistical Regression Modeling of Glass Properties - Tutorial"; independently peer reviewed paper at:
<http://glassproperties.com/principle/>
- [27] S. G. Loryan, R. S. Saringyulyan, K. A. Kostanyan; Fizika i Khimiya Stekla, vol. 3, 1977, no. 6, p 612.
- [28] R. S. Saringyulyan, K.A. Kostanyan; Arm. Khim. Zh., vol. 23, 1970, no. 10, p 928.
R. S. Saringyulyan, K. A. Kostanyan; in: Stekloobraznoe Sostoyanie, Moskva, 1971, p 289.
R. S. Saringyulyan: Vyazkost i Elektroprovodnost Stekol Sistemy $K_2O-PbO-SiO_2$ v Shirokom Intervale Temperatur; Thesis, Erevan, 1972.
K. A. Kostanyan, R. S. Saringyulyan; Elektrokimiya i Rasplavy, Moskva, 1974, p 193.
R. S. Saringyulyan, K. A. Kostanyan; in: Stekloobraznoe Sostoyanie, Erevan, 1974, p 31.
R. S. Saringyulyan; Elektroprovodnost Stekol v Shirokom Intervale Temperatur. Deposited in VINITI, Moscow, no.902-69 Dep., 1969.
- [29] E. S. Verzhkhovskaya; Vopr.Radioelektron., Ser.4: Tekhnol.Proizv.Oborud., 1961, no. 7, p 10.
- [30] K. Endell, J. Hellbrügge: "Über den Einfluß des Ionenradius und der Wertigkeit der Kationen auf die elektrische Leitfähigkeit von Silikatschmelzen zwischen 1250 und 1450°C (About the influence of the ionic radius and the valency of the cations on the electrical conductivity of silicate melts in the range of 1250°C to 1450°C)"; Glastechn. Ber., vol. 20, 1942, no. 10, p 277-287.
- [31] D. G. Montgomery: "Design and Analysis of Experiments", John Wiley & Sons, 2001.
- [32] S. Dowdy and S. Wearden: "Statistics for Research", John Wiley & Sons, 1983.
- [33] R. H. Myers, D. C. Montgomery: "Response surface methodology"; 2nd edition, John Wiley & Sons, Inc. 2002.
- [34] J. A. Cornell: "Experiments with Mixtures - Designs, Models and the Analysis of Mixture Data"; Wiley Series in Probability and Statistics; Wiley-Interscience; 3rd Edition, January 2002, ISBN: 0-471-39367-3.
- [35] N. R. Draper, H. Smith: "Applied regression analysis", John Wiley & Sons, 1998.
- [36] A. P. Dempster: "Elements of Continuous Multivariate Analysis"; Addison-Wesley, New York, New York, 1969.
- [37] J. Neter, M. H. Kutner, W. Wasserman, Ch. J. Nachtsheim: "Applied Linear Regression Models"; 3rd Edition, McGraw-Hill/Irwin, 1996, ISBN: 025608601X.
- [38] Resistivity calculation software available at <http://glassproperties.com/resistivity/>
- [39] A. Fluegel, A. K. Varshneya, D. A. Earl, T. P. Seward, D. Oksoy: "Improved Composition-Property Relations in Silicate Glasses, Part I: Viscosity"; Ceramic Transactions, vol. 170, "Melt Chemistry, Relaxation, and Solidification Kinetics of Glasses" - Proceedings of the 106th Annual Meeting of the American Ceramic Society, 2005, p 129-143.
- [40] A. Fluegel, D. A. Earl, A. K. Varshneya, T. P. Seward: "Statistical analysis of glass melt properties for high accuracy predictions: Density and thermal expansion of silicate glass melts"; Proceedings CD, DGG Meeting, Würzburg, Germany, May 23-25, 2005.

- [41] C. J. R. Gonzalez-Oliver, P. S. Johnson, P. F. James: "Influence of water content on the rates of crystal nucleation and growth in lithia-silica and soda-lime-silica glasses"; *J. Mater. Sci.*, vol. 14, no. 5, 1979, p 1159.
- [42] E. M. Birtch, J. E. Shelby: "Effect of water in the melting atmosphere on the transformation temperature of commercial glasses"; *Ceramic Transactions*, vol. 141, The American Ceramic Society, 2004, p 347-354.
- [43] D. B. Rapp, J. E. Shelby: "Water diffusion and solubility in soda-lime-silica melts"; *Phys. Chem. Glasses*, vol. 44, no. 6, 2003, p 393-400.
- [44] J.-H. Hwang, J.-H. Park, K. D. Kim, S.-S. Choi: "Influence of mixed alkali oxides on some melt properties of TV screen glass"; *Glass Sci. Technol. Glastechn. Ber.*, vol. 73, Jan 2000, no. 1, p 8-17.
- [45] M. Tomozawa: "Alkali ionic transport in mixed alkali glasses"; *J. Non-Cryst. Solids*, vol. 152, 1993, p 59-69.
[http://dx.doi.org/10.1016/0022-3093\(93\)90444-3](http://dx.doi.org/10.1016/0022-3093(93)90444-3)
- [46] O. V. Mazurin, E. S. Borisovskii; *Soviet Phys.-Tech. Phys.*, vol. 2, 1957, p 243.
Citation and ternary diagram also in: J. O. Isard: "The mixed alkali effect in glass"; *J. Non-Cryst. Solids*, vol. 1, 1969, p 235-261.
- [47] J. O. Isard: "Electrical conduction in the aluminosilicate glasses"; *J. Soc. Glass Technol.*, vol. 43, 1959, p 113T-123T.